Fuel 368 (2024) 131652

Contents lists available at ScienceDirect

Fuel

journal homepage: www.elsevier.com/locate/fuel

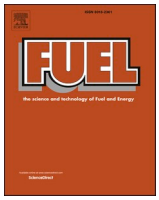

Full Length Article

Predictive models of laminar flame speed in $NH_3/H_2/O_3$/air mixtures using multi-gene genetic programming under varied fuelling conditions

Zubair Ali Shah, G. Marseglia *, M.G. De Giorgi *

University of Salento, Dep. Engineering for Innovation, Via per Monteroni 73100, Lecce, Italy

ARTICLE INFO

Keywords:
NH_3
H_2
Laminar Flame Speed (LFS)
Ignition Delay Time (IDT)
Ozone (O_3)
Multi-gene genetic programming

ABSTRACT

The primary aim of this study is to develop and validate a novel multi-gene genetic programming approach for accurately predicting Laminar Flame Speed (LFS) in ammonia (NH_3)/hydrogen (H_2)/air mixtures, a key aspect in the advancement of carbon-free fuel technologies. Ammonia, particularly when blended with hydrogen, presents significant potential as a carbon-free fuel due to its enhanced reactivity. This research not only investigates the effects of hydrogen concentration, initial temperature, and pressure on LFS and Ignition Delay Time (IDT) but also explores the impact of oxidizing agents like ozone (O_3) in augmenting NH_3 combustion. A modified reaction mechanism was implemented and validated through parametric analysis.

Main findings demonstrate that IDT decreases with higher hydrogen concentrations, increased initial temperature, and initial pressure, although the influence of pressure decreases above 10 atm. Conversely, at lower temperatures (below 1200 K) and higher hydrogen concentrations (30 % and 50 %), the dominance of H_2 chemistry can negatively impact initial pressure. LFS increases with higher temperature and hydrogen concentration, but decreases under elevated pressure, with its effect becoming negligible above 5 atm. An optimized equivalence ratio (Φ) range of 1.10 – 1.15 is identified for efficient combustion. Introducing ozone into the oxidizer notably improves LFS in NH_3/H_2/air mixtures, with the addition of 0.01 ozone mirroring the effect of a 10 % hydrogen addition under normal conditions.

The study's fundamental contribution is the development of a multi-gene genetic algorithm, showcasing the correlation between predicted LFS values and actual values derived from chemkin simulations. The successful validation of this methodology across various case studies underscores its potential as a robust tool in zero-carbon combustion applications, marking a significant stride in the field.

1. Introduction

The ecological consequences of human actions on the heightened levels of greenhouse gases (GHGs) and the growing concern on the climate change issue have recently prompted research into low or zero-emission alternative solutions as systems employing biofuels or alternative fuels [1–5]. In the current worldwide scenario, the optimization of performance and the reduction of pollutants emissions from aviation transportation are important priorities, a consequence of the spreading concern about the availability of fossil fuel reserves and the focus on finding alternative fuels with high thermal efficiency and clean emission characteristics, as H_2 or NH_3 [6–9].

H_2 is considered a highly promising clean fuel due to its exceptional energy density per unit of mass and absence of carbon-relative pollutant emissions [10]. Currently, most of the hydrogen production process relies on fossil fuels, which can release carbon dioxide (CO_2) as a byproduct, and the overall environmental impact may not be as 'clean' as one might expect. However, there is a growing effort to produce green hydrogen through methods like electrolysis powered by renewable energy sources (i.e. solar, wind, etc.) which has the potential to be a clean and sustainable fuel. Airbus has introduced the "ZEROe" project, with the objective to create in 2035 the first commercial aircraft with zero emissions [11]. For this kind of aircraft, powered by modified gas turbine engines, the purpose is to use liquid H_2-like fuel [12]. Despite its growing recognition as a fuel, molecular H_2 still faces significant limitations due to its high volatility and flammability. These drawbacks include the requirement for specialized infrastructure, as well as the associated costs and safety concerns related to storage and transportation. Nevertheless, the production capacity of H_2 still requires further development in order to entirely replace conventional fossil fuels [13]. In this context, a practical approach to gradually enhance the

* Corresponding authors.
E-mail addresses: guido.marseglia@unisalento.it (G. Marseglia), mariagrazia.degiorgi@unisalento.it (M.G. De Giorgi).

https://doi.org/10.1016/j.fuel.2024.131652
Received 19 November 2023; Received in revised form 28 January 2024; Accepted 3 April 2024
Available online 8 April 2024

Nomenclature

Acronyms

ANN	Artificial Neural Networks
CHBR	Close Homogeneous Batch Reactor
GA	Genetic Algorithm
GHGs	greenhouse gases
GP	Genetic Programming
HC	Hydrocarbons
IDT	Ignition Delay Time
LFS	Laminar Flame Speed
LHV	Lower Heating Value
LBV	Laminar burning velocity
MAE	Mean absolute error
MGGP	Multi-gene genetic programming
ML	Machine Learning
MSE	Mean squared error
PLFSR	Premixed Laminar Flame Speed Reactor
RMSE	Root-Mean-Squared Error
SSE	Sum Squared Error
OPSF	Outwardly propagating spherical flame

Symbol

Φ	Equivalence ratio
P	Pressure (atm)
P_0	Ambient pressure (1 atm)
R^2	Coefficient of determination
T	Temperature (K)
T_0	Ambient Temperature (298 K)

combustion performance and minimize pollutant production in aircraft engines is to blend H_2 with other alternative fuels, for example, methane (CH_4), and NH_3 [6,14]. Recently, many researchers and companies have moved their interest surrounding NH_3 as a carbon-free alternative fuel·NH_3 presents a relatively high energy density of 13 MJ/l. It can be conveniently stored in a liquid state under a pressure of 1.1 MPa at a temperature of 300 K [15]. Furthermore, NH_3 exhibits a Lower Heating Value (LHV), reaching 18.8 MJ/kg. Despite that, due to the high corrosiveness and toxicity of NH_3 in real applications, it is essential to utilize rigorous protection and prevention procedures, particularly in real applications for operators. Considering these factors, various recent studies have been conducted to investigate the effects of NH_3 on main combustion efficiency, considering various current challenges related to its main combustion parameters, chemical kinetics modeling, and its utilization as fuel in real transport systems [16,17]. However, a significant limitation of NH_3 as a fuel is its notably low combustion intensity. Thus, the improvement of the LFS in practical combustion systems using NH_3 represents today an interesting research issue for many scientists [18,19].

Considering the need to combine NH_3 in a mixture, it is important to consider that the ignition energies of NH_3 must be deeply greater than traditional fossil fuels. One of the most common issues due to the low LFS values of NH_3/air mixtures, combined with the floating effect, is the occurring phenomenon of the propagation of a spherical flame that propagates outwards (OPSF) [20,21]. This results in the loss of its spheric shape and affects the accuracy of experimental measurement methodologies. In these optical, operating parameters, such as Φ, IDT, LFS, inlet pressure, and temperature strongly affect the combustion behavior and need optimization to allow for achieving high performance and minimizing the emissions. Numerous experimental studies have explored the improvement of combustion by introducing H_2 as a seed into NH_3. Lee et al. [22] performed a comprehensive study on laminar premixed H_2-added NH_3/air flames for H_2 production. They focused on examining the combustion features at various Φ and for different H_2 fractions within the fuel blend considered. Gotama et al. [23] investigated the Laminar Burning Velocity (LBV) behavior and Markstein length of NH_3/H_2/air premixed flames at intermediate H_2 ratio in the binary fuel for different pressures and Φ. In order to optimize the modeling of the flame, they developed an optimized mechanism using the measurement of the LFS. Ichikawa et al. [24] examined the LBV and Markstein length of stoichiometric NH_3/H_2/air mixtures using the OPSF method at 298 K but with different initial pressures. Han et al. [25] investigated the relation between temperature dependence and the LBV for NH_3/air flames. In their research, they based their kinetic simulations on different literature mechanisms developed for NH_3 combustion. Lesmana et al [26] conducted an experimental and kinetic modeling study of LFS in mixtures of partially dissociated NH_3 in air. In order to provide LFS, they considered different CHEMKIN modeling including three different reaction mechanisms, the Okafor [27], Otomo [28], and Mathieu and Petersen [29] mechanisms, respectively. The presence of H_2 resulted in an augmentation of crucial radicals such as OH, H, O, and NH_2, consequently promoting the transformation of NH_2 into NH, HNO, and NNH. This led to a notable upsurge in the LFS. Pessina et al. [30] analyzed the LFS correlations for NH_3/H_2/air mixtures at elevated pressures, considering the range of 40–130 bar and high temperatures for the range from 720 K to 1200 K, for various Φ (0.4–1.5). They utilized an extensive dataset of chemical kinetics simulations considering various blends of NH_3 and H_2 (ranging from 0 to 100 mol% H_2 in increments of 20).

Many researchers are moving their attention to the effect of oxygen (O_2) addition in NH_3/H_2 mixtures. Mei et al. [31] developed a kinetic model to analyze the effects of O_2 enrichment, Φ, and initial pressure on the laminar flame evolution of NH_3. They proved that the O_2 addition can enhance flame propagation and reduce the buoyancy effect. Sreshta et al. [32] examined the laminar flame speeds of NH_3 with O_2-enriched air (with oxygen content ranging from 21 to 30 vol%) and NH_3/H_2-air mixtures (with fuel H_2 content varying from 0 to 30 vol%) at high pressure (1–10 bar) and temperature (298–473 K) values.

Currently, another important challenge is represented by the effects of O_3 addition on combustion features improvement [33].

Ozone is typically generated using corona discharge, ultraviolet radiation, or electrolysis. Corona discharge is the most widely used method for industrial-scale ozone generation, where an electric discharge is used to split oxygen molecules (O_2) into individual oxygen atoms [34]. These atoms can then combine with O_2 molecules to form ozone (O_3). Recent advancements in this technology focus on enhancing energy efficiency and reducing nitrogen oxide by-products. Integrating ozone into combustion systems requires careful consideration of the ozone's point of entry and the control of its concentration. The method of integration varies based on the combustion system's design and the specific objectives of ozone addition, such as improving flame speed or reducing emissions. Advances in control systems and sensors are crucial for accurately monitoring and adjusting ozone levels in real-time to optimize combustion processes.

Wang et al. [35] investigated the combustion improvement using ozone additives for CH_4/air flames through the measurement of LBV and the development of kinetic modeling. Chen et al. [36] analyzed the impact of ozone addition on the LBV of premixed flames consisting of NH_3/(35 %O_2/65 %N_2) and $NH_3 + CH_4/C_2H_6/C_3H_8$ + air. Their studies considered a wide range of Φ. The introduction of O_3 had notable effects, such as decreasing the ignition energy and increasing the burning velocities of the entire mixture when NH_3 was blended with hydrocarbons (HC). This finding holds significance in the development of NH_3 co-firing mechanisms involving diverse complex fuels, thus validating the

feasibility of NH_3 utilization in practical applications. The combined effects of zero-carbon fuel mixture composition and ozone seeding on combustion remain unclear but assume fundamental importance in optimizing and assessing the combustion in a large range of operating conditions. On the other hand, the ozone addition can allow for the reduction of NOx formation in combustion processes [37,38].

In modern research, Machine Learning (ML) methods have gained increasing significance, offering the potential to unravel these intricate interactions and improve our understanding of combustion processes. For instance, ML techniques such as Artificial Neural Networks (ANN) have been successfully applied in studying combustion, flame dynamics, and ignition processes [39,40]. The utilization of ANN offers promising capabilities in non-linear regression, tabulation, and order reduction. This, in turn, enables improved prediction accuracy with reduced memory and CPU-time requirements [41]. Furthermore, ANN can be effectively employed for analyzing experimental measurements [39,42]. Echard et al. [43] compared multiple machine-learning techniques for the calculation of LBV for H_2-CH_4 mixtures. Also Wan et al. [44] developed an optimal ML model to evaluate the LFS of single hydrocarbon and oxygenated fuel with simple descriptors.

This study analyses the LFS and IDT of the NH_3/H_2/air mixtures and investigates the effect of the addition of O_3 in the oxidizer at different Φ. With the objective of assessing combustion evolution, a new modeling of LFS and IDT is developed in the CHEMKIN environment [45]. Firstly, the effects of H_2 enrichment (range from 0 % to 50 %) for NH_3/H_2/air mixtures are examined and discussed. Secondly, the effects of initial pressure and initial temperature on IDTs and the influence of initial pressure, temperature, and Φ on LFS are underlined. Finally, the behavior of LFS for different O_3 content in the oxidizer in terms of mole fraction (0–0.01) of NH_3/H_2/air mixtures at various Φ, at constant pressure and temperature conditions is analyzed.

This study presents a novel and comprehensive approach to predicting Laminar Flame Speed (LFS) in NH_3/H_2/air mixtures, marking a significant advancement in the field of carbon-free fuel technologies. At the heart of its innovation is the development of a multi-gene genetic programming method, a groundbreaking tool in the predictive modeling of LFS. This method accurately correlates predicted LFS values with actual values derived from Chemkin simulations, showcasing its robustness and precision.

Focusing on NH_3/H_2 blends, the research delves into a relatively underexplored yet promising area in carbon-free fuels. The study's comprehensive analysis extends beyond standard parameters like hydrogen concentration, initial temperature, and pressure, to include the impact of oxidizing agents such as ozone (O_3) on combustion dynamics. This approach not only provides a detailed understanding of NH_3/H_2/air mixtures but also opens up new avenues for optimizing combustion processes.

By implementing and validating a modified reaction mechanism through extensive parametric analysis, the research underscores its commitment to detailed and accurate exploration. This approach ensures that the findings are not only theoretically sound but also practically relevant, particularly in identifying optimized combustion conditions such as the equivalence ratio (Φ) range.

The multi-gene genetic programming approach introduced in this study significantly advances the modeling of Laminar Flame Speed (LFS) in ammonia/hydrogen mixtures, a complex task involving intricate chemical interactions. This method stands in contrast to conventional models such as chemical kinetic modeling, empirical correlations, computational fluid dynamics (CFD), simplified analytical models, and traditional machine learning techniques. Unlike these standard approaches, which may struggle with the non-linear relationships inherent in combustion processes, the multi-gene genetic programming technique proficiently handles these complexities. It offers a more dynamic analysis by integrating NH_3, H_2, and O_3, shedding light on the nuanced effects these components have on LFS.

The incorporation of ozone into NH_3 and H_2 combustion mixtures marks a unique aspect of this research. Traditional methods have not extensively explored ozone's role as an oxidizing agent in altering combustion dynamics, particularly in NH_3/H_2 blends. This study's use of multi-gene genetic programming effectively reveals how ozone impacts combustion characteristics, providing novel insights. This approach not only deepens the understanding of combustion processes but also suggests new ways to use ozone in enhancing combustion efficiency and effectiveness.

2. Methodology

A comprehensive evaluation of NH_3 combustion mechanisms is performed to modify the mechanism and perform the parametric study. From the comprehensive review of the Mei mechanism [31] is selected for the modification and performs the parametric study because the Mei model more precisely captured the LFS and IDT [31,46] within the experimental uncertainties. In addition, the Mei mechanism was proven to be more precise in predicting NO experimental findings in a jet-stirred reactor [47]. Therefore, the Mei mechanism was chosen as the reference combustion mechanism in this study for further modification and validation. The modified mechanism is validated against various conditions for IDT and LFS, then performed the simulation to study the effect of different key parameters on the LFS and IDT of the $NH_3/H_2/O_3$/Air mixture. Finally, the study introduces a multi-gene genetic programming technique for predicting LFS in diverse $NH_3/H_2/O_3$/Air conditions, while taking into account factors such as H_2 concentration, initial temperature, and pressure.

2.1. Details of the combustion kinetic mechanism

For $NH_3/H_2/O_3$/Air mixtures, the combustion mechanism proposed by Mei et al. [31] was modified and validated. This mechanism integrates the H_2-based mechanism from Hashemi et al. [48]. Additionally, a number of chemically termolecular reactions that are essential for the LFS predictions of H_2 (H + O_2 + O/OH/H = products) that were left out of the H_2 mechanism from Hashemi et al. [48] are included in the base H_2 model, the NH_3 sub-mechanism from Shrestha et al. [49].

In the present work the excited species reactions of O (^{1}D), O_2 ($a^1\Delta_g$), which have a positive effect on the LFS introduced by Konnov [50], were added to the base mechanism and also O_3 sub-mechanism reactions present in Table 1 were included from ZH Wang et al. [35] to the base mechanism to investigate the effect of ozone, further details of the mechanism can be found in the [31].

In this study, two different reactor models were employed to analyze the combustion process: the Premixed Laminar Flame Speed Reactor (PLFSR) and the 0D Closed Homogeneous Batch Reactor (CHBR). The

Table 1
Modified O_3 sub-mechanism integrated into the Mei-Mech [31].

NO.	Reaction	A	E	N
1.	$O_3 + O_2 \rightarrow O_2 + O + O_2$	1.54E + 14	23,064	0
2.	$O_3 + O \rightarrow O_2 + O + O$	2.48E + 15	22,727	0
3.	$O_3 + N_2 \rightarrow O_2 + O + N_2$	4.00E + 14	22,667	0
4.	$O_3 + O_3 \rightarrow O_2 + O + O_3$	4.40E + 14	23,064	0
5.	$O_2 + O + O_2 \rightarrow O_3 + O_2$	3.26E + 19	0	−2.1
6.	$O_2 + O + O \rightarrow O_3 + O$	2.28E + 15	−1391	−0.5
7.	$O_2 + O + N_2 \rightarrow O_3 + N_2$	1.60E + 14	−1391	−0.4
8.	$O_2 + O + O_3 \rightarrow O_3 + O_3$	1.67E + 15	−1391	−0.5
9.	$O_3 + H \rightleftharpoons O + HO_2$	4.52E + 11	0	0
10.	$O_3 + H_2O \rightleftharpoons O_2 + H_2O_2$	6.62E + 01	0	0
11.	$O_3 + NO \rightleftharpoons O_2 + NO_2$	8.43E + 11	2603	0
12.	$O_3 \rightleftharpoons O_2 + O$	4.31E + 14	22,300	0
13.	$O_3 + N \rightleftharpoons O_2 + NO$	6.00E + 07	0	0
14.	$O_3 + O \rightleftharpoons O_2 + O_2$	4.82E + 12	4094	0
15.	$O_3 + H \rightleftharpoons O_2 + OH$	8.430E + 13	934	0
16.	$O_3 + OH \rightleftharpoons O_2 + HO_2$	1.85E + 11	831	0
17.	$O_3 + HO_2 \rightleftharpoons OH + O_2 + O_2$	6.62E + 09	994	0

modeling of Laminar Flame Speed (LFS) and Ignition Delay Time (IDT) was conducted using the respective PLFSR and CHBR modules within the CHEMKIN software.

The PLFSR model focuses on a freely propagating premixed flame. This model presumes an adiabatic, one-dimensional flame and utilizes premixed $NH_3/H_2/N_2$/air mixtures, integrating multicomponent transport properties. It also operates under the assumption that the impact of radiative heat loss on the flame is negligible, as supported by findings from Nakamura and Shindo (2019) which suggest that the reduction in flame speed due to radiative heat loss is minor and falls within the uncertainty range of standard measurements [51]. The initial conditions for the PLFSR simulations were set at a temperature of 298 K and a pressure of 1 atm. The calculation was performed by solving the governing equations through the Newton iteration algorithm. This method was used to ascertain the eigenvalue of the problem, which effectively corresponds to the laminar burning flux.

The IDT, on the other hand, was estimated using CHEMKIN's Closed Homogeneous Batch Reactor model, which maintains a constant volume. In this context, the simulated IDT is defined as the duration from the start of the simulation to the point where the maximum rate of change in OH concentration is observed. In the CHBR solver, the relative and absolute error tolerance in the ODEs solver is set to be $1.0e^{-6}$ and $1.0e^{-12}$.

All simulations within these models produced grid-independent solutions, ensuring the reliability and accuracy of the computational findings in assessing both LFS and IDT under the specified conditions.

2.2. Validation

To validate the updated combustion mechanism, we utilized both experimental results from studies by Han et al. [52], Ichikawa et al. [24], and Charles et al. [53], as well as simulation results from works by Okafor et al. [27], San Diego et al. [54], and Tian et al. [55]. Specifically, we correlated the Laminar LFS of stoichiometric NH_3/H_2/air flames across a H_2 blend range from 0 % to 60 %, as illustrated in Fig. 1.

Fig. 1 highlights that the calculated LFS values from the present and San Diego models agree with the experimentally measured data for specific conditions. However, it's notable that the Okafor and Tian model performs well up to a 20 % H_2 concentration but consistently underestimates LFS in all other scenarios.

Figs. 2(a)–(d) show a comparison between the predictions of the present model and other models against experimental IDT data [14] for NH_3/H_2 mixtures at $\Phi = 1.0$ and pressures of 1.2 atm and 10 atm. In the

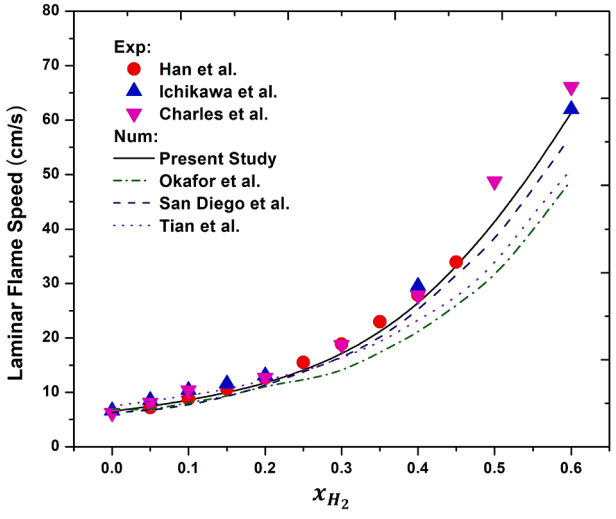

Fig. 1. LFS of stoichiometric NH_3/H_2/air mixtures, as a function of x_{H_2}, Symbols signify the experiment data, whereas lines show the simulated findings of the current model and prior models at P = 1 atm and T = 298 K.

case of the pure NH_3 mixture (0·.04375NH_3/ 0.03281O_2/ 0.92344Ar), as illustrated in Fig. 2(a) and 2(b), the current model, along with the Zhang Model [56], Otomo Model [28], Mathieu Model [29], and Glabrog Model [57], all yield reasonable predictions for IDTs at 1.2 atm and 10 atm.

The Okafor Model [24] significantly overestimated the IDTs at both 1.2 atm and 10 atm. However, it consistently gives accurate predictions for NH_3 flame speed and NO concentration within the flames. This model is constructed upon the GRI 3.0 model [58] and incorporates NH_3 oxidation kinetics from Tian et al. [55].

The Nakamura Model [59] significantly underestimated the IDT at 10 atm. In agreement with the research conducted by Miller and Bowman [60], NH_3-related chemistry underwent re-evaluation, drawing from numerous literature investigations. The chemistry of N_2H_x was based on the research of Konnov et al. [61,62]. It's worth noting that this model exhibited considerable variation in its ability to predict IDT results due to its evaluation limited to species profiles of O_2, NH_3, NO, N_2O, and H_2O under atmospheric pressure in a weak flame.

The Stagni Model [63] provided faster but significantly underestimated Ignition Delay Times (IDTs) at pressures of 1.2 atm, while it overestimated IDTs at 10 atm and above 1450 K. The chemistry related to $HONO/HNO_2$ was derived from a theoretical investigation by Chen et al. [64], and the nitrogen chemistry in the model was based on the research by Song et al. [65].

In Figs. 2(c) and (d), with a 30 % H_2 blend in the NH_3/H_2 mixture (0·.03322NH_3/ 0.01424H_2/0.03203O_2/ 0.92051Ar), both the present model and the Otomo model reliably predict IDTs at 1.2 atm and 10 atm. The Glarborg Model accurately anticipates IDTs for NH_3/H_2 blends at 1.2 atm but somewhat underestimates them at 10 atm.

The shorter ignition delay time for NH_3/H_2 mixtures at 10 atm compared to 1.2 atm is a result of a combination of factors. These include increased reaction rates due to higher molecular collision frequency, elevated temperatures enhancing chemical reactions, favourable formation of reactive intermediates, reduced heat loss, and improved mixing of reactants due to enhanced molecular interactions. Each of these factors plays a critical role in the complex dynamics of combustion at varying pressures.

3. Results and discussion

3.1. Effect of H_2 enrichment in the NH_3/H_2/air mixture on LFS and IDT

LFS is a critical combustion parameter, representing the rate at which the normal flame front advances relative to the unburned mixture.

LFS is frequently used to validate combustion kinetic models, a crucial consideration in the design of practical combustion systems·NH_3 is known for its slower flame speed compared to H_2 and hydrocarbon fuels, making it necessary to advance our understanding of how various parameters, including additives, influence NH_3 flame speed to facilitate effective NH_3 oxidation.

Another key element in premixed combustion is the IDT, which represents the duration it takes for a mixture to auto-ignite. Understanding IDT is essential for both theoretical research and for addressing ignition behavior, whether normal or anomalous, in real-world combustion systems. IDT can be determined by observing the time at which a particular species' concentration reaches its peak or when the temperature reaches its inflection point. In this study, IDT is defined as the time at which a specific rate of temperature rise occurs.

The analyzed hydrogen concentration range up to 50 % aims to explore the impact of hydrogen's reactivity on combustion, particularly on ignition and flame stability, while also considering safety concerns like boundary layer flashback. This range reflects practical scenarios, from hydrogen as a minor additive to a major component, in line with the shift towards hydrogen-based energy systems. Similarly, the pressure range of 1 to 30 atm covers conditions from ambient to industrial

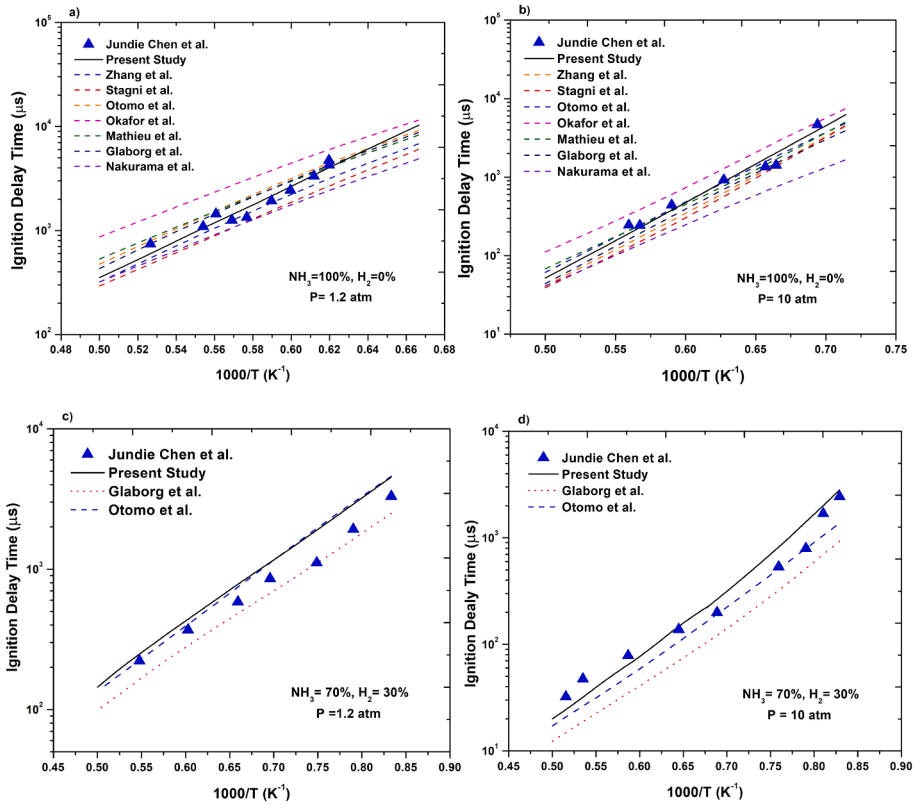

Fig. 2. Relationships between the experimental and model-predicted IDTs of stoichiometric NH_3/H_2 mixtures using present and other models at pressures of 1.2 atm and 10 atm.

settings, crucial for understanding NH3/H2 mixtures' combustion dynamics. This broad pressure spectrum helps identify safe and efficient operational limits and aligns with standard pressures in combustion research, enhancing comparative analysis and insights into these mixtures under various conditions.

Fig. 3 shows the effect of H_2 enrichment and Φ on the LFS of NH_3/H_2/air mixture at P = 1 atm and T = 298 K. By increasing the concentration of H_2 in the NH_3/H_2/air mixture, the flame speed increases significantly and non-linearly. This behaviour can be due to hydrogen's substantially higher reactivity and flame speed than NH_3. As NH_3 is steadily replaced by H_2, the latter takes over as the dominant oxidant.

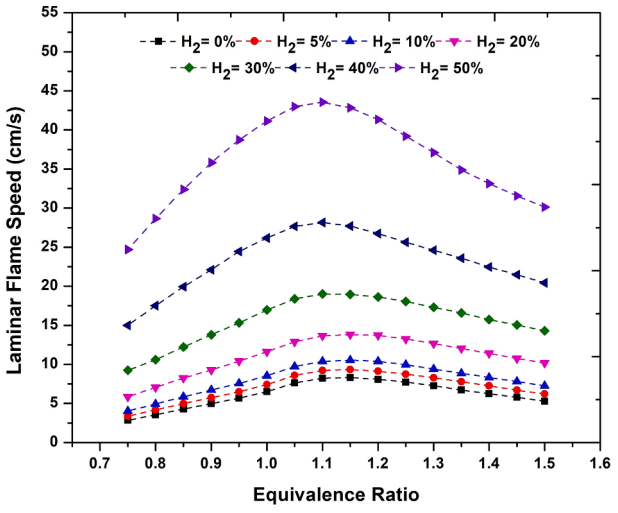

Fig. 3. Effect of H_2 enrichment and Φ of NH_3/H_2/air mixtures on the LFS at P = 1 atm and T = 298 K.

However, large H_2 concentrations in NH_3/H_2/air mixture should be avoided since hydrogen's strong reactivity might cause boundary layer flashback [66]. Furthermore, the flame speed grows consistently at fuel-lean conditions, peaks when the Φ is around 1.1–1.15, and subsequently decreases at fuel-rich conditions.

In the presence of 40 % and 50 % H_2 in the mixture, the maximum LFS reaches approximately 29 cm/s and 44 cm/s, respectively, at Φ of 1.1. To provide context, pure methane burns at a premixed flame speed of about 37 cm/s [27] under identical conditions, while pure H_2 burns at a premixed flame speed of above 200 cm/s [24]. This suggests that using an NH_3/H_2/air mixture with an Φ of 1.1–1.15 is a viable approach to achieve stable combustion in the combustor.

Fig. 4 shows the IDT as a function of H_2 concentration in NH_3/H_2/air mixtures at 1 atm, Φ = 1.0, and temperatures ranging from 1000 K to 2000 K. As evident in Fig. 4, IDT decreases as the H_2 concentration in the mixture increases from 0 % to 50 %. Specifically, when the H_2 concentration in the mixture approaches 50 %, the IDT reduces from approximately 2222 ms to about 1.1 ms at 1000 K and from around 3 ms to roughly 0.05 ms at 1500 K. This indicates that incorporating a more reactive fuel component into NH_3 significantly reduces the IDT, which is advantageous for achieving robust ignition.

3.2. *Effect of initial pressure on LFS and IDT of NH_3/H_2/air mixture*

Fig. 5 illustrates the impact of the initial pressure of NH_3/H_2/air mixtures on the LFS at 298 K and various Φ. With increasing initial pressure, the laminar flame speed decreases. Higher pressures result in a thicker flame and a slower burning speed. The influence of initial pressure is more pronounced at pressures up to 5 atm in all scenarios, while the effect diminishes at higher pressures.

In the case of pure NH_3/air case (H_2 = 0 %) at Φ = 1 and Φ = 1.1 the LFS decreases from 6.5 cm/s to 4.4 cm/s and 8.1 cm/s to 5.8 cm/s when pressure decreases from 1 atm to 5 atm, whereas it decreases from 4.4

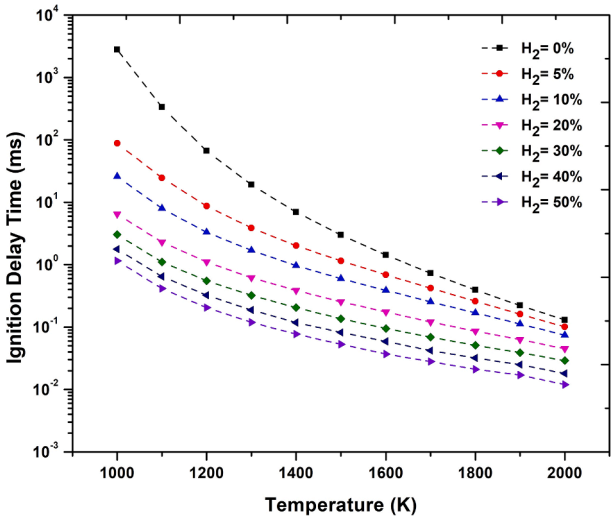

Fig. 4. Effect of H_2 enrichment of NH_3/H_2/air mixtures on IDT at $\Phi = 1$, P = 1 atm.

cm/s to 3.7 cm/s and 5.8 cm/s to 5 cm/s when pressure decreases from 5 atm to 10 atm, respectively.

In the case of 30 % of H_2 in the mixture at $\Phi = 1$ and $\Phi = 1.1$ the LFS decreases from 16.9 cm/s to 9.7 cm/s and 19 to 12.1 cm/s when pressure decreases from 1 atm to 5 atm, whereas it decreases from 9.7 cm/s to 7.9 cm/s and 12.1 cm/s to 10 cm/s when pressure decreases from 5 atm to 10 atm, respectively. This means that the LFS is less sensitive to initial pressure under high-pressure situations, which are more common in engine operating settings.

Figs. 6 (a)–(d) demonstrate the impact of initial pressure (ranging from 1 atm to 30 atm) on the IDT of stoichiometric NH_3/H_2/air mixtures with H_2 concentrations of 0, 10, 30, and 50 %, across temperatures from 1000 K to 2000 K. As depicted in Figs. 6 (a) and (b), for mixtures containing 0 % and 10 % H_2, an increase in initial pressure shortens the IDT within the temperature range of 1000 K to 2000 K. However, the rate of reduction diminishes as the initial pressure continues to rise. When the initial pressure exceeds 10 atm, the influence of initial pressure on ignition delay becomes marginal.

The initial pressure demonstrates a negative effect on the IDT in the temperature range of 1000 K to 1100 K for the cases of 30 % and 50 % H_2 in the stoichiometric NH_3/H_2/air mixtures, as indicated in Figs. 6(c) and (d). In the case of 30 % and 50 % H_2 in the mixture, the IDTs can be shortened only at high temperatures (T > 1200 K), whereas at lower temperatures, the IDTs can become significantly longer.

The impact of initial pressure on the IDT is observed to have a negative effect within the temperature range of 1000 K to 1100 K for the scenarios involving 30 % and 50 % H_2 in the stoichiometric NH_3/H_2/air mixtures, as depicted in Figs. 6(c) and (d). It's worth noting that for these blends the reduction in IDTs is only significant at high temperatures (T > 1200 K), while at lower temperatures, the IDTs can become notably longer.

The negative pressure dependence indicated above was also studied in the literature with respect to the ignition delays of H_2-enriched hydrocarbons [36,67–71]. When the H_2 concentration is sufficiently high, the H_2 chemistry dominates the ignition delays of the dual mixture [69–71].

3.3. Effect of initial temperature on LFS of NH_3/H_2/air mixture

Fig. 7 shows that as the initial temperature of the mixture rises, the LFS also increases, and this pattern is consistent across all cases, with the highest value falling within the Φ range of 1.1–1.15. At a Φ of 1.15, the LFS increases from approximately 8.1 cm/s to about 20 cm/s when the initial temperature of the mixture is raised from 298 K to 473 K.

NH_3/H_2/air mixtures follow the same behaviour as NH_3/air mixtures in increasing the initial temperature, and the maximum value for LFS

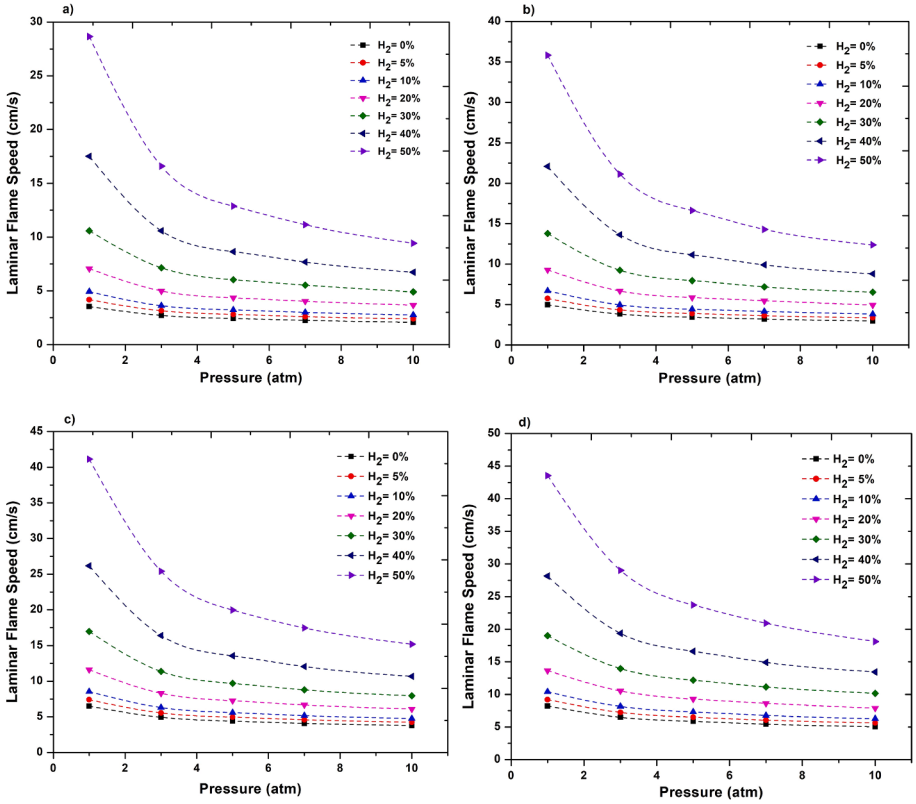

Fig. 5. Effect of initial pressure on LFS of NH_3/H_2/air mixtures at different Φ a) $\Phi = 0.8$b) $\Phi = 0.9$c) $\Phi = 1.0$ d) $\Phi = 1.1$ and P = 1 atm, T = 298 K.

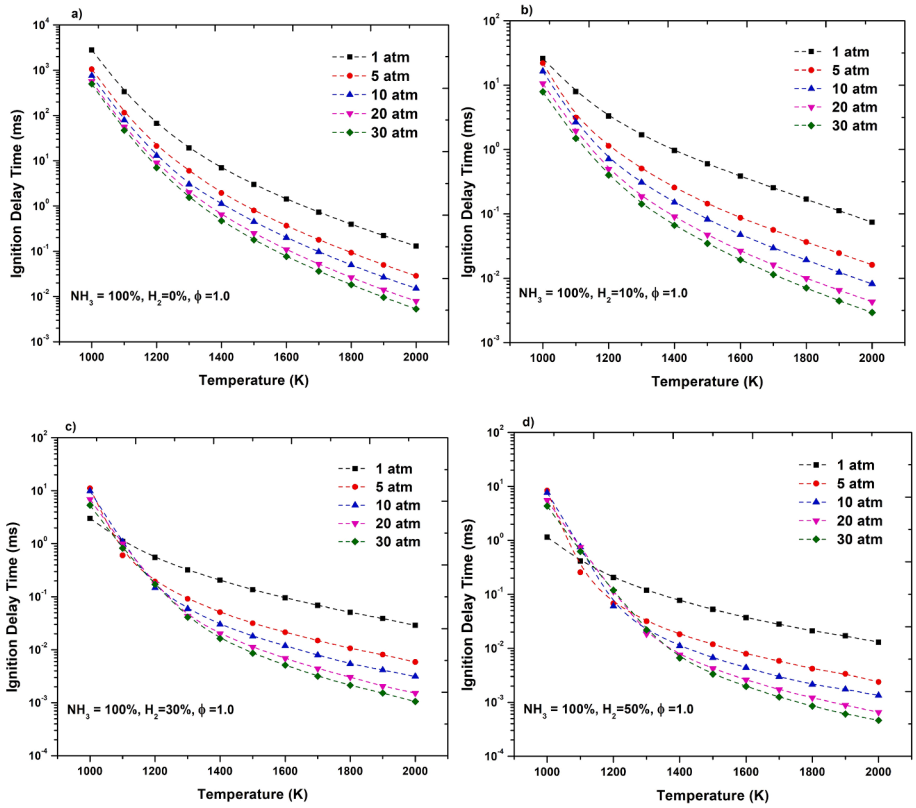

Fig. 6. Effect of initial pressure on IDT of stoichiometric NH_3/H_2/air mixtures a) $H_2 = 0$ %, b) $H_2 = 10$ %, c) $H_2 = 30$ %, d) $H_2 = 50$ % at the temperature ranging from 1000 K to 2000 K.

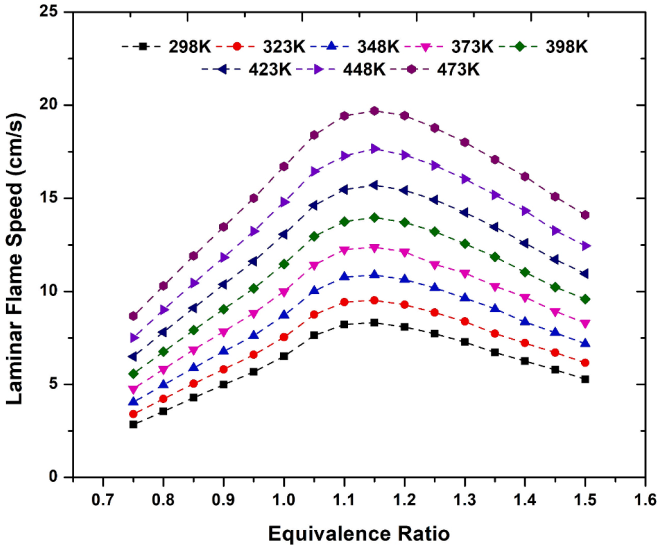

Fig. 7. Effect of initial temperature and Φ on LFS of NH_3/air mixtures at P = 1 atm.

lies in the equivalence range of 1.1–1.15, as shown in Figs. 8 (a)–(d). For H_2 blends of 5 % (Fig. 8a), 10 % (Fig. 8b), 30 % (Fig. 8c), and 50 % (Fig. 8d), the LFS increases at $\phi = 1.15$, and it rises from 9.4 cm/s to 22 cm/s, 10.5 cm/s to 24.5 cm/s, 19 cm/s to 43 cm/s, and 43.5 cm/s to 95.4 cm/s for each respective H_2 blend.

The distinctive properties of H_2 play a key role in accelerating the laminar flame speed, especially when it's part of a mixture with NH_3. One of the most achieving features of hydrogen is its high reactivity. Thanks to its wide flammability range and relatively low ignition energy, H_2 sets the stage for rapid chemical reactions. This becomes particularly evident in its interaction with other gases like ammonia, where its presence significantly speeds the combustion process, thereby increasing the speed at which the flame front propagates.

Moreover, hydrogen's remarkably low molecular weight marks it as one of the lightest gases available. This characteristic bestows upon H_2 a superior diffusivity, enabling its molecules to move and intermingle with air or other oxidizers much more rapidly than heavier molecules. This efficient mixing is crucial; it enhances the overall combustion process, facilitating a quicker advancement of the flame.

Another key aspect is hydrogen's high heat of combustion. When H_2 burns, it releases a considerable amount of energy, elevating the temperature of the flame. It's a well-known fact that higher flame temperatures are synonymous with increased reaction rates, which in turn, speed up the flame's progression.

Additionally, the activation energy required for H_2 combustion is notably lower compared to many other fuels. This lower threshold means that the necessary reactions for combustion are more easily initiated and proceed at a faster pace, further boosting the flame speed.

Hydrogen's role becomes even more pronounced when considering its effect on turbulent mixing. The addition of hydrogen to the mixture can significantly alter the physical dynamics of turbulence. This enhanced turbulence, in turn, leads to a more efficient rate of heat and mass transfer, all contributing to a faster-moving flame front.

Lastly, the very presence of H_2 in an NH_3/H_2 mix alters the traditional combustion mechanisms. Hydrogen actively engages in chain-branching reactions, a critical component in the propagation of flames. These reactions facilitate a more effective and efficient combustion process, ultimately leading to an increase in the laminar flame speed.

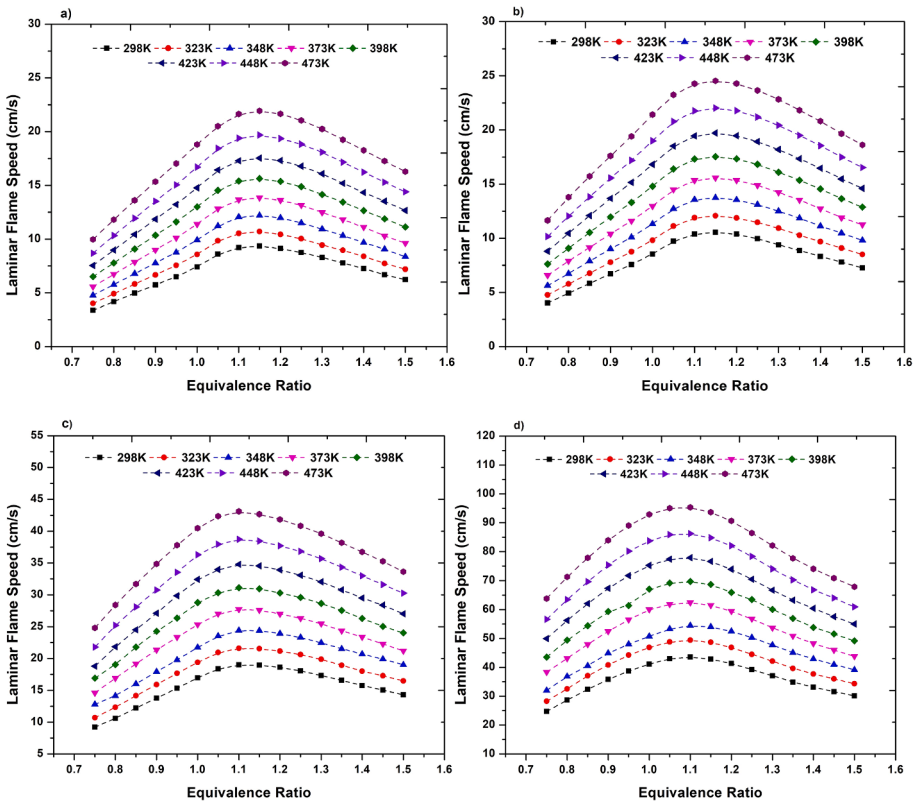

Fig. 8. Effect of initial temperature and ϕ on LFS at different H_2 concentrations a) $H_2 = 5$ %, b) $H_2 = 10$ %, c) $H_2 = 30$ %, d) $H_2 = 50$ % at P = 1 atm.

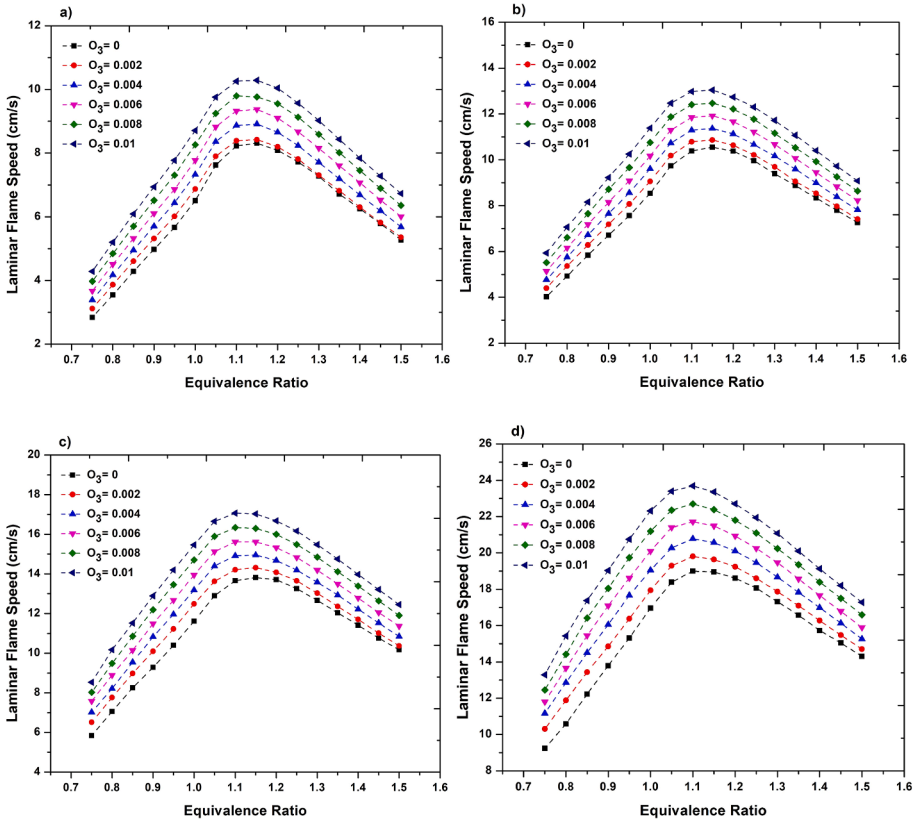

Fig. 9. Effect of O_3 and ϕ on LFS of NH_3/H_2/air mixtures at different H_2 concentrations a) $H_2 = 0$ %, b) $H_2 = 10$ %, c) $H_2 = 20$ %, d) $H_2 = 30$ % and P = 1 atm, T = 298 K.

3.4. Effect of O_3 on LFS of NH_3/H_2/air mixture

Previous research has shown that adding O_3 to hydrocarbon fuels improves LFS. Wang et al. [35] used a heat flux burner and found that injecting 3730 ppm O_3 at stoichiometric conditions increased the LFS of CH_4/air by 3.5 %. X Gao et al.[72] investigated the effect of O_3 on LFS experimentally and numerically utilizing three fuels, CH_4, C_2H_4, and C_3H_8, over a wide pressure range and found that for a stoichiometric CH_4/air mixture with 6334 ppm O_3 addition, the improvement in the measured flame speed increased from 7.7 % at atmospheric pressure to 11 % at 2.5 atm. Ombrello et al. [73] showed a 4 % increase in LFS of C_3H_8 /air in stoichiometric lifted flames. Weng et al. [74] reported a stronger effect in fuel-rich mixes than in stoichiometric mixtures. The improvement in LFS is intimately linked to the chemistry of ozone, particularly the fast exothermic ozonolysis reactions that involve unsaturated hydrocarbons and the decomposition of O_3 to form atomic oxygen. However, no such investigations on NH_3/H_2/air mixtures with O_3 addition have been conducted.

Fig. 9 shows the effect of the O_3 concentration in the oxidizer in terms of mole fraction (0 – 0.01) on the LFS at various H_2 concentrations (0–30 %) and ϕ of NH_3/H_2/air mixtures at a pressure equal to 1 atm, and temperature equal to 298 K.

Ozone generation using plasma discharge [34], typically yields ozone concentrations that can vary significantly depending on various factors such as the type of plasma generator, discharge power, and gas flow rates. These concentrations usually range from a few parts per million (ppm) to several thousand ppm. The range of 0–0.01 mol fraction considered in the present study likely corresponds to this practical and achievable spectrum for plasma discharge systems, making it relevant for experimental and real-world applications.

Furthermore the range is comparable to those used in other research involving different fuel/air mixture, i.e. CH_4/air [35,72].

Enhancing the oxidizer by increasing the concentration of O_3 from 0 to 0.01 markedly improves the laminar flame speed (LFS) across all cases, an observation that underscores the critical role of ozone in the combustion process. This enhancement can be attributed to the conversion of ozone into oxygen, which effectively raises the concentration of atomic oxygen (O). This additional oxygen plays a significant role in the chemical processes involving ammonia, leading to an increased rate of ammonia oxidation and overall improvement in combustion efficiency.

The impact of this ozone enhancement on the LFS is most notable within a specific range of equivalence ratios (Φ), particularly between 1.1 and 1.15. In this range, the LFS demonstrates its peak values, reflecting the optimum conditions for combustion. For instance, in the absence of hydrogen (pure NH_3/air mixture), the LFS sees an increase from 8.1 cm/s to 10.28 cm/s as shown in Fig. 10. Similarly, with incremental additions of H_2 — 10 %, 20 %, and 30 % — the LFS values show a corresponding rise from 10.5 cm/s to 13.04 cm/s, 13.8 cm/s to 17.07 cm/s, and 18.99 cm/s to 23.69 cm/s, respectively. These increases highlight the profound effect of integrating ozone into the oxidizer mix.

Furthermore, the role of hydrogen in this context cannot be overstated. Hydrogen's unique characteristics, including its high reactivity, minimal weight, substantial energy output, reduced requirement for activation energy, and its significant impact on combustion dynamics, collectively contribute to its status as a transformative element in combustion processes. When H_2 is combined with NH_3, it significantly enhances the combustion efficiency, which is further augmented with each increase in ozone concentration. This synergy between H_2 and O_3 in the presence of NH_3 leads to a notable acceleration in the flame speed, demonstrating the intricate interplay of these components in optimizing combustion.

4. Genetic programming

In this study, multi-gene genetic programming (GP) was employed to accurately predict the laminar flame speed under various fuel mixture conditions.

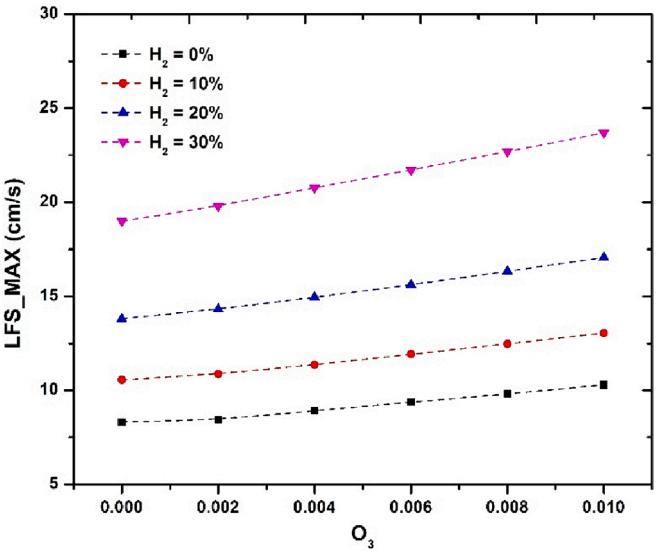

Fig. 10. Effect of ozone in the oxidizer in terms of mole fraction on maximum LFS of NH_3/H_2/air at normal conditions.

Genetic Programming (GP) and Genetic Algorithm (GA) are both subfields of evolutionary computation (EA), but they have distinct characteristics and applications.

The main difference between genetic algorithms (GAs) and genetic programming (GP) lies in the core nature of their components. GAs represent individuals as unchangeable symbolic strings with fixed dimensions, similar to chromosomes. In contrast, in GP, individuals manifest as a wide array of non-linear entities, featuring variations in both magnitude and complex configuration. These entities dynamically evolve, resulting in intricate parse trees. This innovative approach opens new dimensions for evolutionary exploration [75].

In genetic programming (GP), key components include arithmetic functions, decision variables, and evolutionary operators like reproduction, crossover, and mutation. These elements form initial symbolic expressions, establishing the algorithm's initial population. The process uses a tree-based method combining arithmetic functions with decision variables.

During iterations, the algorithm refines this population based on fitness, using genetic operators. Reproduction selects the fittest individuals, crossover mixes parts of two 'parent' individuals to create 'offspring,' and mutation introduces random changes. This cycle continues until reaching a predefined endpoint, such as a maximum number of generations or an error threshold.

In the reproduction phase of genetic programming, the best-performing segment of the population is retained to form a new generation through genetic manipulations. During crossover, pairs of individuals are selected and combined at random points in their structure, creating new 'offspring'. The population is then updated with these new individuals. This process repeats iteratively until a termination criterion, like a maximum number of generations or an error threshold, is met.

GP stands as a symbolic modeling technique of the metaheuristic kind, which forges problem-solving equations guided by the principles of Darwinian natural selection, specifically the concept of 'survival of the fittest' [76]. Presented below is the fundamental structure of the anticipated process model: (Equation (1):

$$y = f(X, \beta) \tag{1}$$

the symbol "f" signifies a non-linear function, characterized by parameters articulated through a P-dimensional vector, denoted as ($\beta[\beta_1, \beta_2, \ldots, \beta_K]^P$). When presented with input and output variables, the GP

Table 2
GP run parameters.

Run parameter	Value
Population size	300
Max. generations	500
Generations elapsed	500
Input variables	2
Nodes	40
Training instances	3992
Tournament size	10
Rain Elite fraction	0.15
Lexicographic selection pressure	On
Probability of pareto tournament	0
Max. genes	4
Crossover probability	0.84

algorithm dynamically adjusts its functional configuration and parameter vector β to align with the provided dataset.

Multi-gene genetic programming (MGGP) is a novel approach that enhances the precision of Genetic Programming by using multiple trees to represent a model, as opposed to the single tree used in conventional GP. Each tree in MGGP, akin to a mathematical expression, contributes to a more intricate and accurate prediction of the output. [77].

MGGP differs from conventional GP by allowing users to precisely set key parameters, like the maximum number of genes and their depth. This control significantly influences the complexity and efficiency of the resulting model, with studies showing MGGP's enhanced accuracy and computational efficiency over traditional GP. [78].

The development of the GP-based model was facilitated by the use of the open-source GPTIPS toolkit and custom-coded subroutines in MATLAB 2019a [76]. The framework adopted in this study encompassed the utilization of the Root-Mean-Squared Error (RMSE) between actual and predicted outcomes as the designated fitness function. The effort was dedicated to minimizing the RMSE value, thereby optimizing the model's predictive performance.

It's important to note that this method is both non-parametric, as it doesn't rely on a predefined functional model, and data-driven, as the optimal model is exclusively determined by the data.

The GP was used to perform a multi-gene genetic programming approach, enabling accurate prediction of laminar flame speed. This prediction was achieved using the dataset from Chemkin, encompassing data for freely propagating laminar flames.

A crucial aspect of our approach was the data partitioning strategy. After extensive testing with various split ratios for dividing the dataset into training and testing sets, it was determined that an 80:20 split ratio is the most effective for the model in question. This decision was reached following a series of experiments where different ratios, ranging from 60:40 to 90:10, were evaluated. In each instance, the model's performance was closely monitored, with particular attention paid to its ability to generalize on unseen data while avoiding overfitting. The choice of the 80:20 split emerged as the optimal balance, ensuring sufficient training data to learn effectively while providing a substantial testing set for a reliable evaluation of the model's performance.

Table 2 provides an overview of the model parameters.

Different conditions have been analyzed, as follows:

- Case A: Pure ammonia at ambient conditions (298 K, 1 atm) and different ϕ.
- Case B: Pure ammonia at different ϕ, ambient pressure and 298 K.
- Case C: Blend NH_3/H_2 at different ϕ and H_2 fraction at ambient conditions (298 K, 1 atm).
- Case D: Blend NH_3/H_2 at different ϕ and ambient pressure at 298 K.
- Case E: Blend NH_3/H_2 at different ϕ, ambient pressure and temperature.
- Case F: Blend NH_3/H_2 at different ϕ, with air and O_3 addition.
- Case G: Blend NH_3/H_2 at different ϕ, H_2, pressure, temperature, and with air and O_3 addition.

Case A: Pure ammonia at ambient conditions (298 K, 1 atm) and different ϕ.

The following equation was selected as the best model for the LFS in the case of pure ammonia at ambient conditions:

$$LFS = \phi*3.26e^{2} + exp(-\phi^{3})*3.23e^{2} - exp(-\phi^{6})*4.64e^{1} - \phi^{3}*log(\phi)*5.41e^{1} - 4.21e^{2}$$

In the study, the effectiveness of the multi-gene genetic programming model is quantitatively showcased in Table 3, which details the model's performance metrics during both the training and testing phases. Additionally, Fig. 11a graphically represents the correlation between measured and predicted values of laminar flame speed (LFS) for the test dataset. The strength of this correlation is quantified by the coefficient of determination, R2, which is remarkably high in both examined scenarios, underscoring the model's accuracy.

Specifically, for Case A, which examines pure ammonia at ambient conditions (298 K, 1 atm) across various equivalence ratios (Φ), the R2 value reaches an impressive 0.9975. This near-perfect correlation indicates an extremely high level of precision in the model's predictions under these standard environmental conditions.

On the other hand, Case B, which involves pure ammonia with varying Φ at a constant temperature of 298 K and ambient pressure, shows a slightly lower, yet still significantly high, R^2 value of 0.990. This indicates that while there is a slight decrease in predictive accuracy compared to Case A, the model still maintains a strong predictive capability in this scenario.

These R2 values, particularly the exceptionally high value in Case A, demonstrate the robustness and reliability of the multi-gene genetic programming approach in predicting LFS under varying conditions. The minor difference in the R2 values between the two cases also provides valuable insights into the model's performance under different sets of combustion conditions, highlighting its comprehensive applicability in combustion research.

Case B: Pure ammonia at different ϕ, pressure and 298 K.

The optimal model chosen for the LFS with pure NH_3/air mixtures at different Φ and pressure and ambient temperature is represented by the following equation:

$$LFS = \phi*5.42 - exp(\phi*6.36 + \phi^{2}*3.0)*3.35e^{-5} + exp(exp((P/P0)* - 7.58e^{-1})* - 1.0)*3.64 + (\phi^{2}*1.23e^{1})/abs(\phi + (P/P_0)) + \phi^{5}*2.71 - 6.13$$

Table 3 displays the metrics obtained from both the training and testing phases. Additionally, Fig. 11b provides a visual representation of the comparison between the LFS values that were found with chemkin and those that were predicted specifically for the test dataset by GP. The results distinctly indicate a robust association between the forecasted information generated by the multi-gene model and the target data.

Case C: Blend NH_3/H_2 at different ϕ and H_2 fraction at ambient conditions (298 K, 1 atm).

The laminar flame speed for freely propagating laminar flames at 298 K and 1 atm and different ϕ and H_2 content (from 0 to 100) was found. The best model is given by the following equation:

$$LFS = 315.0tanh(\phi^{2}) + 419.0(2.0\phi + X_{H2})^{1/2} - 416.0(\phi + X_{H2} - 1.0exp(-1.0\phi))^{1/2} + (1.3e^{16}X_{H2} + 1.64e^{16})/(3.52e^{13}\phi + 1.76e13X_{H2} + 1.74e^{13}) - 813.0$$

Table 3
Metrics for LFS Predictions for different conditions.

Metric	CASE A	CASE B	CASE C	CASE D	CASE E	CASE F	CASE G
Training							
R^2	0.99773	0.99134	0.99976	0.99638	0.98794	0.98061	0.98647
RMSE	0.071081	0.20848	0.70069	2.7601	11.0105	18.1117	15.0216
MAE	0.059015	0.1278	0.4469	1.865	8.199	12.6419	10.771
SSE	3.8399	32.9902	1959.918	24896.63	165359.2	1177969.46	810304.1037
Max. abs. Error	0.16079	4.0464	6.1563	27.5005	85.0807	116.0078	200.9182
MSE	0.005053	0.043465	0.49096	7.6183	121.2311	328.0338	225.6486
Test							
R^2	0.9975	0.98993	0.99972	0.99689	0.98713	0.97751	0.98676
RMSE	0.070845	0.24475	0.75518	2.5729	10.3409	18.7693	14.8683
MAE	0.058827	0.13984	0.45876	1.7811	7.6527	13.2974	10.6677
SSE	0.95863	11.3812	569.7228	5414.809	36571.68	316352.28	198517.7684
Max. abs. error	0.15918	2.6618	6.3697	17.842	54.3409	123.0659	102.8528
MSE	0.005019	0.059901	0.57029	6.6196	106.9347	352.2854	221.0666

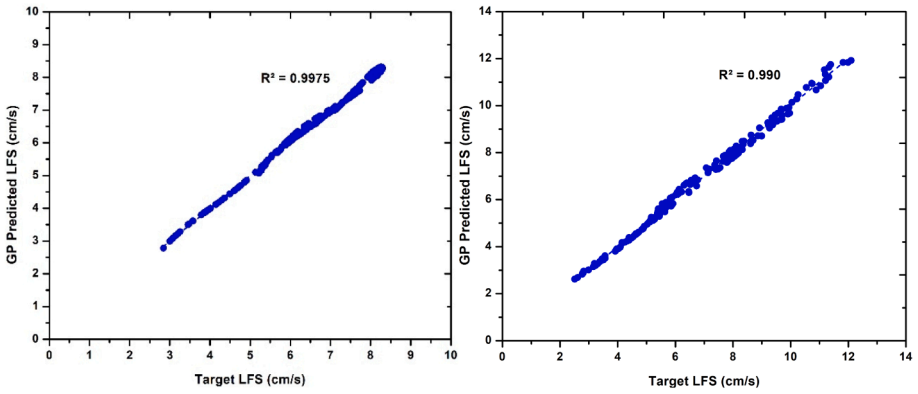

a) CASE A b) CASE B

Fig. 11. Target (Chemkin) versus predicted (multigene GP) data for the LFS for NH_3/ air mixtures at: a) different Φ and P = 1 atm T = 298 K; b) at different Φ and pressure at T = 298 K.

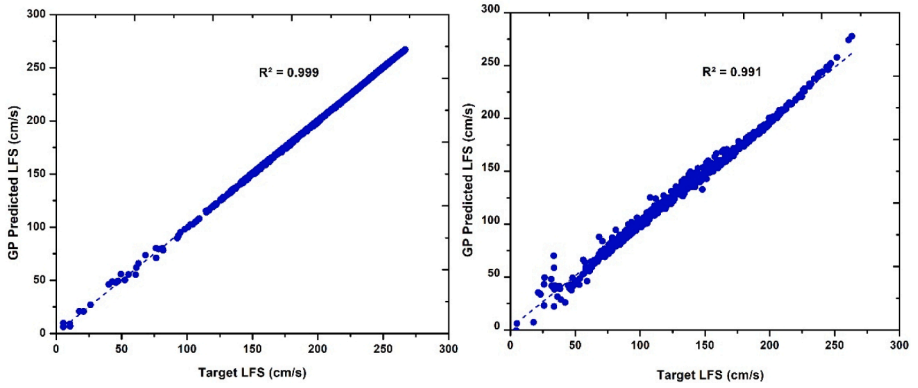

a) CASE C b) CASE D

Fig. 12. Target (Chemkin) versus predicted (multigene GP) data for the LFS for NH_3/ H_2/air mixtures at: a) different Φ and H_2 mass fraction at 298 K and 1 atm, b) different Φ, H_2 mass fraction and pressure at 298 K.

Where X_{H2} is the mass fraction ranging from 0 for pure NH_3 to 100 for pure H_2.

Similar to the previous comparisons, the predictive performance in this case is also favorable. Table 3 presents the metrics acquired during both the training and testing stages. Furthermore, Fig. 12a offers a graphical depiction of the contrast between the LFS values obtained through chemkin and the ones predicted exclusively for the test dataset using GP. The outcomes clearly affirm a strong correlation between the projected insights produced by the multi-gene model and the intended target data.

Case D: Blend NH_3/H_2 at different ϕ and pressure at 298 K.

The laminar flame speed has been investigated for freely propagating laminar flames assuming temperatures from 298 K to 500 K and a pressure range of 1 atm to 30 atm. These investigations encompass various ϕ and H_2 concentrations ranging from 0 to 100. Among the different models examined, the most effective one is depicted by the

subsequent equation:

$$LFS = (5.3e^{15}X_{H2}tanh(log(\phi)))/(1.76e13X_{H2} + 8.8e^{12}P/P_0) - \left(5.23e15(P/P_0)^{1/2}\right)/(8.8e^{12}(P/P_0) + \left(8.8e^{12}X_{H2}\right)/\phi + 8.8e^{12}(P/P_0)^{1/2}) - 90.6log((P/P_0) + 6.9) + (132.0X_{H2}(x3 - 2.03))/((X_{H2} + 8.51)(X_{H2} + (P/P_0) + 10.0)) + 407.0$$

Where X_{H2} is the mass fraction ranging from 0 for pure NH_3 to 100 for pure H_2 and P/P_0 is the ratio between the pressure and the ambient pressure at 1 atm.

The predictive performance remains promising in this instance as well. Table 3 showcases the metrics gathered from both the training and testing phases. Additionally, Fig. 12b provides a visual representation highlighting the distinction between the target LFS values and those exclusively forecasted for the test dataset utilizing GP. The results undeniably underscore a robust correlation between the anticipated insights generated by the multi-gene model and the desired target data.

Case E: Blend NH_3/H_2 at different ϕ, ambient pressure and temperature.

The laminar flame speed has been investigated for freely propagating laminar flames assuming temperatures from 298 K to 500 K and a pressure range of 1 atm to 30 atm. These investigations encompass various Φ and H_2 concentrations ranging from 0 to 100. Among the different models examined, the most effective one is depicted by the subsequent equation:

$$LFS = 0.246log(\phi^3)(log((P/P_0))) - 1.0\phi^3)(X_{H2} + X_{H2}/(P/P_0) + 15.8) - 0.556\phi^3(T/T_0)^2(\phi + X_{H2}) - 31.0log((P/P_0)/(T/T_0))) + 31.0\phi^2(T/T_0)^2log(X_{H2}) + 1.34\phi^2(T/T_0)^2log(X_{H2})((T/T_0) + 4.77)^{1/2}\left(log(X_{H2}) - 1.0(P/P_0)^{1/2}\right) + 105.0$$

Where X_{H2} is the mass fraction ranging from 0 for pure NH_3 to 100 for pure H_2, P/P_0 is the ratio between the pressure and 1 atm and T/T_0 is the ratio between the temperature and 298 K.

The predictive capability continues to show promise in this scenario as well. Table 3 presents the metrics acquired during both the training and testing stages. Furthermore, Fig. 13 underlines the good agreement between the target LFS values and those predicted for the test dataset using GP.

Fig. 14 presents a detailed surface plot that demonstrates how the laminar flame speed (LFS) varies for different NH_3/H_2 blends under a

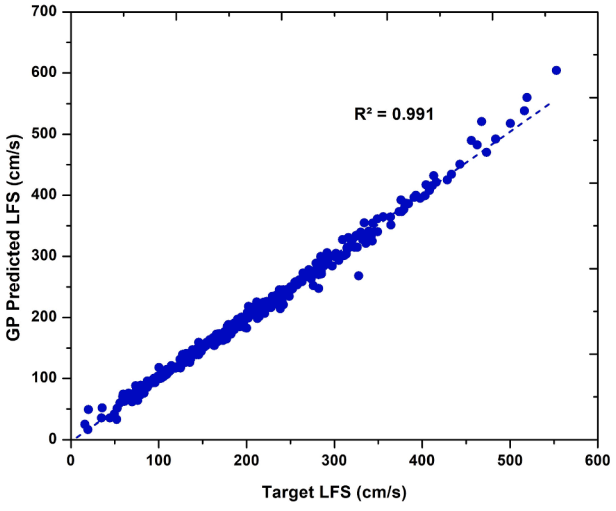

Fig. 13. Target (Chemkin) versus predicted (multigene GP) data for the LFS for NH_3/ H_2/air mixtures at different Φ, H_2 mass fraction, pressure, and temperature.

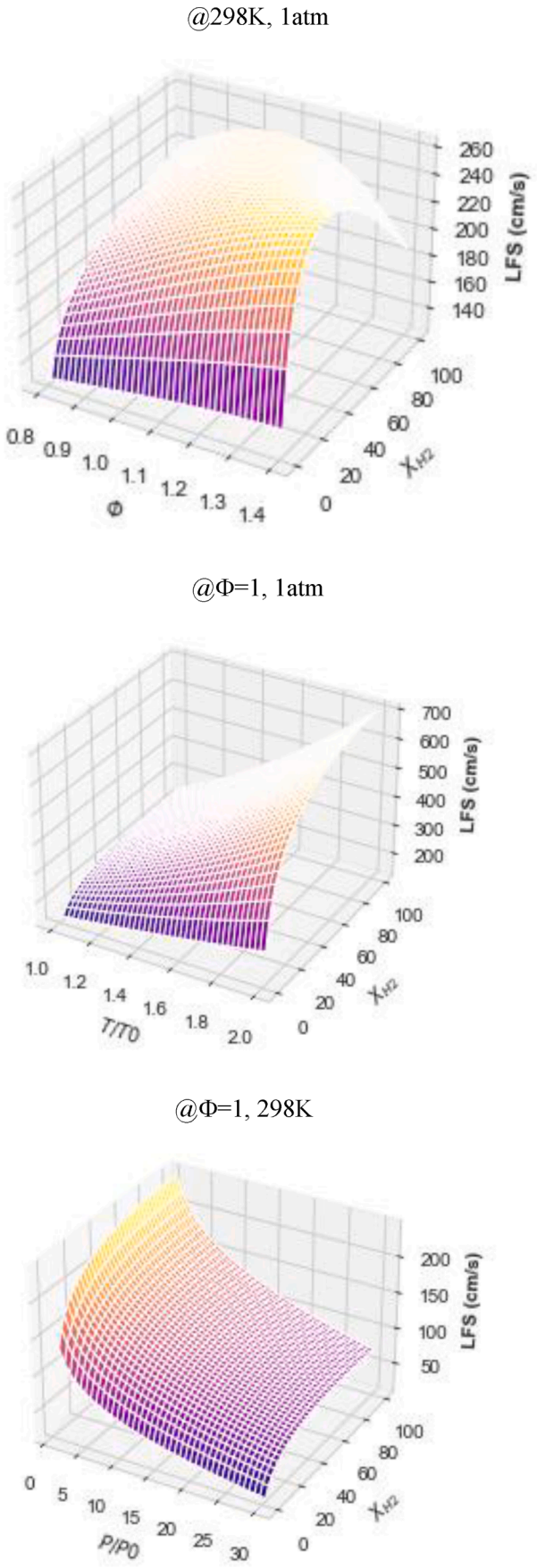

Fig. 14. LFS predicted for NH_3/H_2/air mixtures at different Φ, H_2 mass fraction, pressure, and temperature.

variety of operational conditions, as predicted by our model. This figure effectively highlights the complex relationship between the flame behavior and various operational factors such as pressure, temperature, fuel-to-air ratio, and hydrogen concentration.

In the figure, the first plot at the top depicts the Laminar Flame Speed (LFS) under specific conditions where the pressure is fixed at 1 atm and the temperature at 298 K. In this plot, the variables being explored are the fuel–air ratio and the hydrogen fraction.

The second plot, maintaining a constant pressure of 1 atm and a fuel–air ratio of 1, varies the temperature and the hydrogen fraction. This plot is designed to show the impact of temperature changes and varying hydrogen concentrations on the LFS, while keeping the pressure and fuel–air ratio constant. It provides insights into how temperature and hydrogen content interact and affect the combustion dynamics in the given conditions. Finally, the third plot fixes the temperature at 298 K and the fuel–air ratio at 1, while varying the pressure and the hydrogen fraction. This plot examines the influence of different pressure levels and hydrogen concentrations on the LFS, with all other variables held steady. It helps in understanding the relationship between pressure variations, hydrogen content, and their combined effect on the Laminar Flame Speed in the context of the specified temperature and fuel–air ratio.

Notably, ammonia (NH_3) typically exhibits moderate laminar burning velocities, particularly when contrasted with the faster combustion rates of hydrogen (H_2). The integration of H_2 into NH_3, however, leads to a noticeable enhancement in the LFS of NH_3/air mixtures. This increase in LFS is more pronounced at higher H_2 concentrations. The reason behind this trend can be partly attributed to the increased importance of the H_2-chemistry, especially its chain branching reactions [79], and its inherently high reactivity [80].

This pattern aligns with findings in similar studies, such as those conducted by Di Sarli et al. [81] and Mitu et al. [82], which explored H_2/CH_4/air mixtures. These studies also observed comparable trends in LFS enhancement with varying H_2 concentrations, further validating the patterns seen in our NH_3/H_2 blends. The surface plot in Fig. 14 not only corroborates these findings but also provides a visual representation of how changes in H_2 concentration and other operational variables intricately influence the combustion characteristics of NH_3/H_2/air mixtures.

Case F: Blend NH_3/ H_2/ O_3/air at different ϕ, and O_3 addition at ambient conditions.

The laminar flame speed for freely propagating laminar flames was calculated at 298 K and 1 bar for various Φ and H_2 contents (ranging from 0 to 100), including cases where ozone was introduced. The optimal model identified through Genetic Programming is represented by the following equation:

$$\begin{aligned} LFS = {} & 4149.51*X_{O3} + 200.0*\phi + (4150.51*X_{O3} + 0.77*\phi*X_{H2}/((-X_{O3} \\ & + X_{H2})*(200.0*\phi + 0.386)*(-\phi + X_{H2} + 0.996)*(X_{O3}*\phi + X_{H2} \\ & - 0.507 + 0.0572*X_{H2}^2/\phi)) + 201.0*\phi - X_{H2} + 189.141 \\ & + (5368.05*X_{O3}*\phi*(\phi - X_{H2}) + X_{O3} + 189.14)/(-X_{H2} - 0.52))/(\\ & - X_{H2} - 0.52) \end{aligned}$$

Where X_{H2} is the mass fraction ranging from 0 for pure NH_3 to 100 for pure H_2, X_{O3} is the mass fraction of O_3 with respect to the total oxides fraction ranging from 0 to 0.03.

Metrics obtained in the training and testing stages are presented in Table 3. In this case, as well, the predictive capability continues to show promise. Furthermore, Fig. 15 provides a graphical representation of the difference between the LFS values that were predicted specifically for the test dataset using GP and those that were produced via chemkin. The outcomes clearly confirm a significant relationship between the multigene model's predicted insights and the desired target data.

Case G: Blend NH_3/H_2 at different ϕ, H_2, pressure, temperature, and with air and O_3 addition.

The laminar flame speed has been investigated for freely propagating laminar flames assuming temperatures from 300 K to 500 K, pressure range of 1 atm to 30 atm, and O_3 range of 0–0.03 in the oxidizer. These investigations encompass various Φ and H_2 concentrations ranging from 0 to 100. The optimal model identified through Genetic Programming is represented by the following equation:

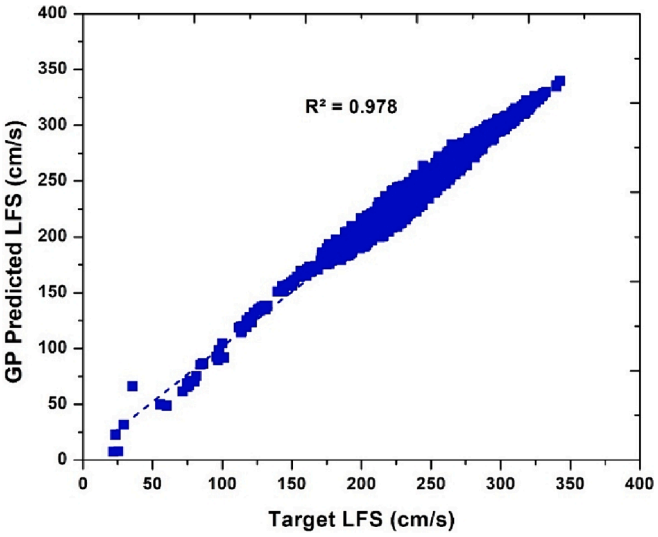

Fig. 15. Target (Chemkin) data versus predicted (multigene GP) data for the LFS for NH_3/ H_2/O_3/air mixtures at different ϕ, x_{H2}, and x_{O3}.

$$\begin{aligned} LFS = {} & 10.6exp(2.0X_{O3} + T/T_0)(2.0X_{O3} + T/T_0 \\ & - 1.0P/P_0^{1/2}) + \Big(0.113P/P_0^{1/2}(P/P_0 \\ & - 1.0X_{H2}T/T_0)\Big)/\phi - 694.0X_{O3}\phi(X_{O3} - 1.0T/T_0)(2.0X_{O3} + T/T_0 \\ & + exp(-1.0\phi) + log(X_{H2})) + 27.8\phi T/T_0 log(3.03X_{H2})(T/T_0 \\ & - 1.0exp(-1.0X_{H2}))) + 70.6 \end{aligned}$$

Where X_{H2} is the mass fraction ranging from 0 for pure NH_3 to 100 for pure H_2, X_{O3} is the mass fraction of O_3 with respect to the total oxides fraction ranging from 0 to 0.03. and P/P_0 is the ratio between the pressure and 1 atm and T/T_0 is the ratio between the temperature and 298 K.

Fig. 16 clearly demonstrates the strong agreement between the target LFS values and those predicted for the test dataset using GP.

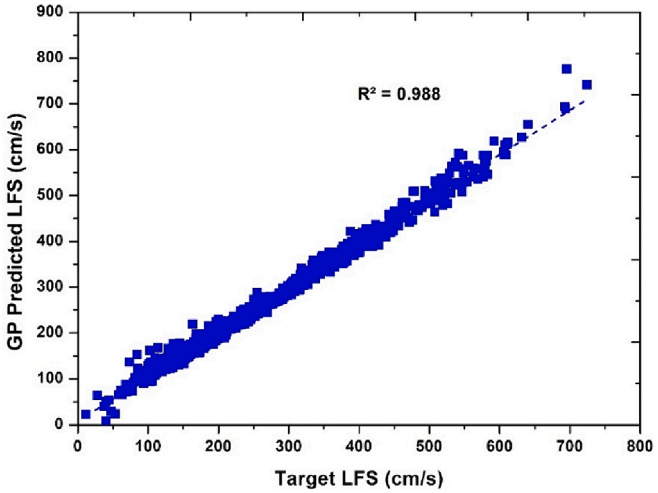

Fig. 16. Target versus predicted (multigene GP) data for the LFS for NH_3/ H_2/ air mixtures at different Φ, H_2 mass fraction, pressure, temperature, and with O_3/air mixture as the oxidizer.

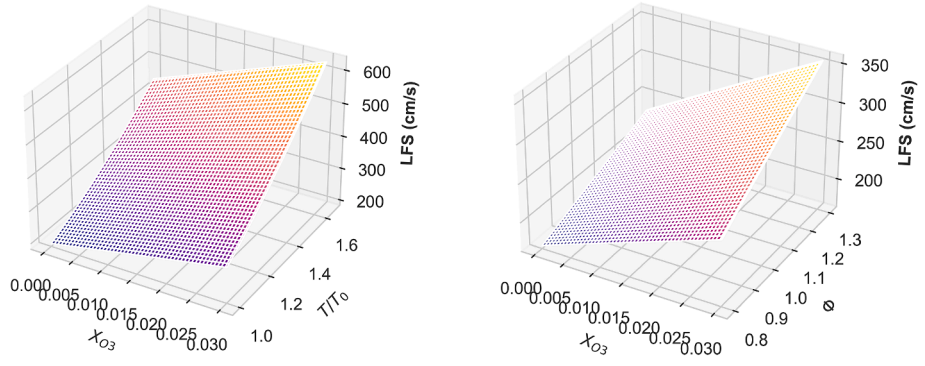

a) b)

Fig. 17. LFS for NH_3/ H_2/O_3/air mixtures at a) different initial temperature and x_{O3}, $\phi = 1$, $x_{H2} = 30$, P = 1 atm b) different x_{O3} and ϕ, $x_{H2} = 30$, P = 1 atm and $T/T_0 = 1$.

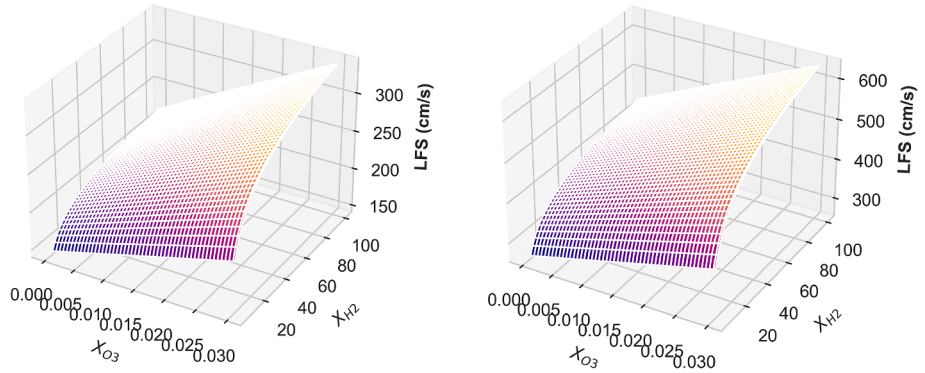

a) b)

Fig. 18. LFS for NH_3/ H_2/O_3/air mixtures at different x_{H2} and x_{O3}, $\phi = 1$, P = 1 atm: a) $T/T_0 = 1$, b) $T/T_0 = 1.5$.

Figs. 17 and 18 present a surface plot depicting LFS for various NH_3/ H_2/O_3/air blends across diverse conditions. This visualization effectively highlights the intricate relationships between flame characteristics and operational parameters, such as temperature, fuel-to-air ratio, O_3, and H_2 concentration. Results show that incorporating a more reactive fuel component into NH_3 such as H_2 and O_3 has a positive effect on the LFS. The addition of 0.01 O_3 in the oxidizer in terms of mole fractions has approximately the same effect as the addition of 10 % H_2 on the LFS of NH_3/air mixture at normal conditions and the improvement of LFS is closely linked to O_3 chemistry, especially fast exothermic ozonolysis reactions and the breakdown of O_3 to form atomic oxygen.

5. Conclusion

In this study, an enhanced NH_3/H_2/Air mechanism was implemented and validated, and a comprehensive parametric analysis was performed. This analysis investigated the effects of various factors such as hydrogen (H_2) concentrations, equivalence ratio (Φ), initial temperature, and initial pressure on laminar flame speed (LFS) and ignition delay time (IDT). Additionally, the impact of ozone (O_3) concentration in the oxidizer, in terms of mole fraction ranging from 0 to 0.01, on the LFS of NH_3/H_2/air mixtures was examined. A significant aspect of the research involved the use of multi-gene genetic programming to accurately predict laminar flame speed under different fuel mixture conditions.

The key findings from this research are as follows:

- It was observed that LFS increases with the rise in H_2 concentration and initial temperature. In contrast, an increase in initial pressure led to a decrease in LFS. Interestingly, at higher pressures (over 5 atmospheres), the effect of initial pressure on LFS lessens, and an optimized equivalence ratio, lying in the range of 1.10 – 1.20, is identified for achieving stable and efficient combustion.
- The study found that IDT decreases with an increase in H_2 concentration, initial temperature, and initial pressure. However, at higher pressures (above 10 atmospheres), the influence of initial pressure on reducing IDT is less pronounced. For mixtures with 30 % and 50 % H_2, the study noted that IDTs could be shortened only at high temperatures (above 1200 K). At lower temperatures, IDTs tend to significantly increase, particularly as the higher H_2 concentration leads to H_2 chemistry dominating the ignition delays in the dual mixture.

- The addition of O_3 to the oxidizer, in mole fractions from 0 to 0.01, was also found to improve the LFS of the NH_3/H_2/air mixture under normal conditions. Adding 0.01 mol fraction of ozone to the oxidizer has approximately the same effect as adding 10 % hydrogen on the LFS of the NH_3/air mixture at normal conditions.
- The predictive capability of the multi-gene genetic programming model developed in this study is promising. This was demonstrated through a comparison between the predicted values using the model and actual values obtained via chemkin simulations, showing a good agreement and confirming the model's accuracy for the examined test dataset.
- The results of this study provide useful insights for the application of numerical machine learning techniques in the field of zero-carbon combustion applications, indicating a significant stride forward in this area.

Looking ahead, there is immense potential for further development in this area. Future works could explore the incorporation of 3D Computational Fluid Dynamics (CFD) analysis simulations, which would provide a more detailed understanding of the combustion processes in green fuels. Such advancements could lead to even more efficient and environmentally friendly combustion technologies, reinforcing the role of green fuels in mitigating the effects of climate change and supporting the transition to a more sustainable energy future.

Funding

This work has been supported under the National Recovery and Resilience Plan (NRRP), Mission 4 Component 2 Investment 1.4—Call for tender No. 3138 of 16 December 2021 of the Italian Ministry of University and Research, financed by the European Union-—NextGenerationEU [Award Number: National Sustainable Mobility Center CN00000023, named MOST, Concession Decree No. 1033 of 17 June 2022, adopted by the Italian Ministry of University and Research, Spoke 14 "Hydrogen and New Fuels".

CRediT authorship contribution statement

Zubair Ali Shah: Writing – original draft, Visualization, Software, Methodology, Data curation. **G. Marseglia:** Writing – review & editing, Writing – original draft, Investigation, Formal analysis. **M.G. De Giorgi:** Writing – original draft, Validation, Supervision, Software, Resources, Methodology, Conceptualization.

Declaration of competing interest

The authors declare that they have no known competing financial interests or personal relationships that could have appeared to influence the work reported in this paper.

Data availability

Data will be made available on request.

References

[1] Islam Rony Z, Mofijur M, Hasan MM, Rasul MG, Jahirul MI, Forruque Ahmed S, et al. Alternative fuels to reduce greenhouse gas emissions from marine transport and promote UN sustainable development goals. Fuel 2023;338:127220. https://doi.org/10.1016/j.fuel.2022.127220.

[2] Ballal V, Cavalett O, Cherubini F, Watanabe MDB. Climate change impacts of e-fuels for aviation in Europe under present-day conditions and future policy scenarios. Fuel 2023;338:127316. https://doi.org/10.1016/j.fuel.2022.127316.

[3] Lu W, Bartocci P, Abad A, Cabello A, de Las Obras Loscertales M, Mendiara T, Wang L, Chen Q, Chen Y, Wang X, Yang H, Chen H, Zampilli M, Fantozzi F. Evaluation of the effect of pressure and heat transfer on the efficiency of a batch fuel reactor, using Iron-based Oxygen Carrier with a CFD model. Fuel 2023; 333, 126266.

[4] Jin S, Wu B, Zi Z, Yang P, Shi T, Zhang J. Effects of fuel injection strategy and ammonia energy ratio on combustion and emissions of the ammonia-diesel dual-fuel engine. Fuel 2023;341:127668. https://doi.org/10.1016/j.fuel.2023.127668.

[5] Novella R, Pastor J, Gomez-Soriano J, Sánchez-Bayona J. Numerical study on the use of ammonia/hydrogen fuel blends for automotive spark-ignition engines. Fuel 2023;351:128945. https://doi.org/10.1016/j.fuel.2023.128945.

[6] Quante G, Bullerdiek N, Bube S, Neuling U, Kaltschmitt M. Renewable fuel options for aviation – A system-wide comparison of drop-in and non-drop-in fuel options. Fuel 2023;333:126269. https://doi.org/10.1016/j.fuel.2022.126269.

[7] Yin F, Gangoli Rao A, Bhat A, Chen M. Performance assessment of a multi-fuel hybrid engine for future aircraft. Aerosp Sci Technol 2018;77:217–27. https://doi.org/10.1016/j.ast.2018.03.005.

[8] Eguea JP, Gouveia P, da Silva G, Martini CF. Fuel efficiency improvement on a business jet using a camber morphing winglet concept. Aerosp Sci Technol 2020; 96:105542. https://doi.org/10.1016/j.ast.2019.105542.

[9] Chai N, Zhou W. A novel hybrid MCDM approach for selecting sustainable alternative aviation fuels in supply chain management. Fuel 2022;327:125180. https://doi.org/10.1016/j.fuel.2022.1251808.

[10] Manigandan S, Praveenkumar TR, Ir Ryu J, Nath Verma T, Pugazhendhi A. Role of hydrogen on aviation sector: A review on hydrogen storage, fuel flexibility, flame stability, and emissions reduction on gas turbine engines. Fuel 2023;352:129064. https://doi.org/10.1016/j.fuel.2023.129064.

[11] Yusaf T, Faisal Mahamude AS, Kadirgama K, Ramasamy D, Farhana K A. Dhahad H, Abu Talib AR. Sustainable hydrogen energy in aviation – A narrative review. International Journal of Hydrogen Energy 2023. DOI: 10.1016/j.ijhydene.2023.02.086.

[12] ZEROe - Low carbon aviation - Airbus, https://www.airbus.com/en/innovation/low-carbonaviation/hydrogen/zeroe#:~:text=In%202022%2C%20we%20launched%20our,combustion%20propulsion%20system%20by%202025, July 2023.

[13] Rondinelli S, Sabatini R, Gardi A. Challenges and benefits offered by liquid hydrogen fuels in commercial aviation, in: Practical Responses to Climate Change (PRCC), Melbourne, Australia, 2014. S. Rondinelli, A. Gardi, R. Kapoor and R. Sabatini. Benefits and challenges of liquid hydrogen fuels in commercial aviation. International Journal of Sustainable Aviation 2017; 3, 200-216. DOI: 10.1504/IJSA.2017.10007966.

[14] Chen J, Jiang X, Qin X, Huang Z. Effect of hydrogen blending on the high-temperature auto-ignition of ammonia at elevated pressure. Fuel 2021;287: 119563. https://doi.org/10.1016/j.fuel.2020.119563.

[15] Lhuillier C, Brequigny P, Lamoureux N, Contino F, Mounaïm-Rousselle C. Experimental investigation on laminar burning velocities of ammonia/hydrogen/air mixtures at elevated temperatures. Fuel 2020;263:116653. https://doi.org/10.1016/j.fuel.2019.116653.

[16] Wu Y, Zhang Y, Xia C, Chinnathambi A, Nasif O, Gavurová B, et al. Assessing the effects of ammonia (NH3) as the secondary fuel on the combustion and emission characteristics with nano-additives. Fuel 2023;336:126831. https://doi.org/10.1016/j.fuel.2022.126831.

[17] Liu Z, Liu F, Wei H, Zhou L. Effects of ammonia addition on knock suppression and performance optimization of kerosene engine with a passive pre-chamber. Fuel 2023;353:129189. https://doi.org/10.1016/j.fuel.2023.129189.

[18] Ju R, Wang J, Zhang M, Mu H, Wu Y, Zhang G, et al. Experimental study on burning velocity, structure, and NOx emission of premixed laminar and swirl NH3/H2/air flames assisted by non-thermal plasma. App Energy Combust Sci 2023;14: 100149. https://doi.org/10.1016/j.jaecs.2023.100149.

[19] Zubair Ali Shah, Ghazanfar Mehdi, Paolo Maria Congedo, Domenico Mazzeo, Maria Grazia De Giorgi. A review of recent studies and emerging trends in plasma-assisted combustion of ammonia as an effective hydrogen carrier. International Journal of Hydrogen Energy 2024; 51, 354-374. DOI: 10.1016/j.ijhydene.2023.05.222.

[20] Han X, Wang Z, He Y, Zhu Y, Lin R, Konnov AA. Uniqueness and similarity in flame propagation of pre-dissociated NH3 + air and NH3 + H2 + air mixtures: An experimental and modelling study. Fuel 2022;327:125159. https://doi.org/10.1016/j.fuel.2022.125159.

[21] Wang S, Elbaz AM, Wang G, Wang Z, Roberts WL. Turbulent flame speed of NH3/CH4/H2/H2O/air-mixtures: Effects of elevated pressure and Lewis number. Combust Flame 2023;247:112488. https://doi.org/10.1016/j.combustflame.2022.112488.

[22] Lee JH, Lee SI, Kwon OC. Effects of ammonia substitution on hydrogen/air flame propagation and emissions. Int J Hydrogen Energy 2010; 35, 11332–41. https://doi. org/10.1016/j.ijhydene.2010.07.104.

[23] Gotama GJ, Hayakawa A, Okafor EC, Kanoshima R, Hayashi M, Kudo T, et al. Measurement of the laminar burning velocity and kinetics study of the importance of the hydrogen recovery mechanism of ammonia/hydrogen/air premixed flames. Combust Flame 2022;236:111753. https://doi.org/10.1016/j.combustflame.2021.111753.

[24] Ichikawa A, Hayakawa A, Kitagawa Y, Somarathne KDKA, Kudo T, Kobayashi H. Laminar burning velocity and Markstein length of ammonia/hydrogen/air premixed flames at elevated pressures. Int J Hydrogen Energy 2015;40:9570–8. https://doi.org/10.1016/j.ijhydene.2015.04.024.

[25] Han X, Wang Z, He Y, Liu Y, Zhu Y, Konnov AA. The temperature dependence of the laminar burning velocity and superadiabatic flame temperature phenomenon for NH3/air flames. Combust Flame 2020;217:314–20. https://doi.org/10.1016/j.combustflame.2020.04.013.

[26] Lesmana H, Zhu M, Zhang Z, Gao J, Wu J, Zhang D. Experimental and kinetic modelling studies of laminar flame speed in mixtures of partially dissociated NH3 in air. Fuel 2020;278:118428. https://doi.org/10.1016/j.fuel.2020.118428.

[27] Okafor EC, Naito Y, Colson S, Ichikawa A, Kudo T, Hayakawa A, et al. Experimental and numerical study of the laminar burning velocity of CH4–NH3–air premixed flames. Combust Flame 2018;187:185–98. https://doi.org/10.1016/j.combustflame.2017.09.002.

[28] Otomo J, Koshi M, Mitsumori T, Iwasaki H, Yamada K. Chemical kinetic modeling of ammonia oxidation with improved reaction mechanism for ammonia/air and ammonia/hydrogen/air combustion. Int J Hydrogen Energy 2018;43:3004–14. https://doi.org/10.1016/j.ijhydene.2017.12.066.

[29] Mathieu O, Petersen EL. Experimental and modeling study on the high-temperature oxidation of ammonia and related NOx chemistry. Combust Flame 2015;162:554–70. https://doi.org/10.1016/j.combustflame.2014.08.022.

[30] Pessina V, Berni F, Fontanesi S, Stagni A, Mehl M. Laminar flame speed correlations of ammonia/hydrogen mixtures at high pressure and temperature for combustion modeling applications. Int J Hydrogen Energy 2020;47:25780–94. https://doi.org/10.1016/j.ijhydene.2022.06.007.

[31] Mei B, Zhang X, Ma S, Cui M, Guo H, Cao Z, et al. Experimental and kinetic modeling investigation on the laminar flame propagation of ammonia under oxygen enrichment and elevated pressure conditions. Combust Flame 2019;210:236–46. https://doi.org/10.1016/j.combustflame.2019.08.033.

[32] Shrestha KP, Lhuillier C, Barbosa AA, Brequigny P, Contino F, Mounaïm-Rousselle C, et al. An experimental and modeling study of ammonia with enriched oxygen content and ammonia/hydrogen laminar flame speed at elevated pressure and temperature. Proc Combust Inst 2021;38:2163–74. https://doi.org/10.1016/j.proci.2020.06.197.

[33] Li Z, Pan J, Zhang F, He Y, Liu C, Wei H. Effects of ozone addition and octane sensitivity on combustion characteristics of gasoline compression ignition engines. Fuel 2023;333:126373. https://doi.org/10.1016/j.fuel.2022.126373.

[34] Gong C, Yu J, Wang K, Liu J, Huang W, Si X, et al. Numerical study of plasma produced ozone assisted combustion in a direct injection spark ignition methanol engine. Energy 2018;153:1028–37. https://doi.org/10.1016/j.energy.2018.04.096.

[35] Wang ZH, Yang L, Li B, Li ZS, Sun ZW, Aldén M, et al. Investigation of combustion enhancement by ozone additive in CH4/air flames using direct laminar burning velocity measurements and kinetic simulations. Combust Flame 2012;159:120–9. https://doi.org/10.1016/j.combustflame.2011.06.017.

[36] Chen C, Wang Z, Yu Z, Han X, He Y, Zhu Y, et al. Experimental and kinetic modeling study of laminar burning velocity enhancement by ozone additive in NH3+O2+N2 and NH3+CH4/C2H6/C3H8+air flames. Proc Combust Inst 2023;39:4237–46. https://doi.org/10.1016/j.proci.2022.07.025.

[37] Nguyen H-T, Domingo P, Vervisch L, Nguyen P-D. Machine learning for integrating combustion chemistry in numerical simulations. Energy and AI 2021;5:100082. https://doi.org/10.1016/j.egyai.2021.100082.

[38] Kuo C-P, Fu JS. Ozone response modeling to NOx and VOC emissions: Examining machine learning models. Environ Int 2023;176:107969. https://doi.org/10.1016/j.envint.2023.107969.

[39] Huang Y, Jiang C, Wan K, Gao Z, Vervisch L, Domingo P, et al. Prediction of ignition delay times of Jet A-1/hydrogen fuel mixture using machine learning. Aerosp Sci Technol 2022;127:107675. https://doi.org/10.1016/j.ast.2022.107675.

[40] Zhou Y, Zhang C, Han X, Lin Y. Monitoring combustion instabilities of stratified swirl flames by feature extractions of time-averaged flame images using deep learning method. Aerosp Sci Technol 2021;109:106443. https://doi.org/10.1016/j.ast.2020.106443.

[41] Wan KD, Barnaud C, Vervisch L, Domingo P. Chemistry reduction using machine learning trained from non-premixed micro-mixing modeling: application to DNS of a syngas turbulent oxy-flame with side-wall effects. Combust Flame 2020;220:119–29. https://doi.org/10.1016/j.combustflame.2020.06.008.

[42] Bhowmick S, Badiwal A, Shenoy KT. Removal of NOx using ozone injection and subsequent absorption in water. Chem Eng J Adv 2023;15:100511. https://doi.org/10.1016/j.ceja.2023.100511.

[43] Eckart S, Prieler R, Hochenauer C, Krause H. Application and comparison of multiple machine learning techniques for the calculation of laminar burning velocity for hydrogen-methane mixtures. Therm Sci Eng Prog 2022;32:101306. https://doi.org/10.1016/j.tsep.2022.101306.

[44] Wan Z, Wang Q-D, Wang B-Y, Liang J. Development of machine learning models for the prediction of laminar flame speeds of hydrocarbon and oxygenated fuels. Fuel Commun 2022;12:100071. https://doi.org/10.1016/j.jfueco.2022.100071.

[45] https://www.ansys.com/it-it/products/fluids/ansys-chemkin-pro.2023.

[46] Taaresh Sanjeev Taneja, PraiseNoah Johnson, Suo Yang. Nanosecond pulsed plasma assisted combustion of ammonia-air mixtures: Effects on ignition delays and NOx emission. Combustion and Flame 2022; 245, 112327.

[47] Sabia P, Manna MV, Cavaliere A, Ragucci R, de Joannon M. Ammonia oxidation features in a jet stirred flow reactor. The role of NH2 chemistry. Fuel 2020;276:118054. https://doi.org/10.1016/j.fuel.2020.118054.

[48] Hashemi H, Christensen JM, Gersen S, Glarborg P. Hydrogen oxidation at high pressure and intermediate temperatures: experiments and kinetic modelling. Proc Combust Inst 2015;35:553–60. https://doi.org/10.1016/j.proci.2014.05.101.

[49] Shrestha KP, Seidel L, Zeuch T, Mauss F. Detailed kinetic mechanism for the oxidation of ammonia including the formation and reduction of nitrogen oxides. Energy Fuels 2018;32:10202–17. https://doi.org/10.1021/acs.energyfuels.8b01056.

[50] Nakamura H, Shindo M. Effects of radiation heat loss on laminar premixed ammonia/air flames. Proc Combust Inst 2019;37:1741–8. https://doi.org/10.1016/j.proci.2018.06.138.

[51] Konnov A. On the role of excited species in hydrogen combustion. Combust Flame 2015;162:3753–70. https://doi.org/10.1016/j.combustflame.2015.07.014.

[52] Han X, Wang Z, Costa M, Sun Z, He Y, Cen K. Experimental and kinetic modeling study of laminar burning velocities of NH3/air, NH3/H2/air, NH3/CO/air and NH3/CH4/air premixed flames. Combust Flame 2019;206:214–26. https://doi.org/10.1016/j.combustflame.2019.05.003.

[53] Lhuilliera C, Brequignya P, Lamoureuxd N, Continoe F, Mounaïm-Rousselle C. Experimental investigation on laminar burning velocities of ammonia/ hydrogen/air mixtures at elevated temperatures. Fuel 2020;263:116653. https://doi.org/10.1016/j.fuel.2019.116653.

[54] "Chemical-Kinetic Mechanisms for Combustion Applications", San Diego Mechanism web page, Mechanical and Aerospace Engineering (Combustion Research), University of California at San Diego (http://combustion.ucsd.edu).

[55] Tian Z,Li Y,Zhang L,Glarborg P,.Qi F. An experimental and kinetic modeling study of premixed $NH_3/CH_4/O_2$/Ar flames at low-pressure Combust Flame 2009; 156, 1413-1426. DOI: 10.1016/j.combustflame.2009.03.005.

[56] Zhang Y, Mathieu O, Petersen EL, Bourque G, Curran HJ. Assessing the predictions of a NO x kinetic mechanism on recent hydrogen and syngas experimental data. Combust Flame 2017;182:122–41. https://doi.org/10.1016/j.combustflame.2017.03.019.

[57] Glarborg P, Miller JA, Ruscic B, Klippenstein SJ. Modeling nitrogen chemistry in combustion. Prog Energy Combust Sci 2018;67:31–68. https://doi.org/10.1016/j.pecs.2018.01.002.

[58] Smith GP, Golden DM, Frenklach M, Moriarty N W, Eiteneer B, Goldenberg M. GRI3. 0 mesh. Gas Research Institute, Chicago, IL, http://www. me. Berkeley. edu/gri_mech.

[59] Nakamura H, Hasegawa S, Tezuka T. Kinetic modeling of ammonia/air weak flames in a micro flow reactor with a controlled temperature profile. Combust Flame 2017;185:16–27. https://doi.org/10.1016/j.combustflame.2017.06.021.

[60] Miller JA, Bowman CT. Mechanism and modeling of nitrogen chemistry in combustion. Prog Energy Combust Sci 1989;15:287–338. https://doi.org/10.1016/0360-1285(89)90017-8.

[61] Konnov AA, Ruyck JDE. Kinetic modeling of the thermal decomposition of ammonia. Combust Sci Technol 2000;152:23–37. https://doi.org/10.1080/00102200008952125.

[62] Konnov AA, De Ruyck J. A possible new route for no formation VIA N_2H_3. Combust Sci Technol 2001;168:1–46. https://doi.org/10.1080/00102200108907830.

[63] Stagni A, Cavallotti C, Arunthanayothin S, Song Yu, Herbinet O, Battin-Leclerc F, Faravelli T. An experimental, theoretical and kinetic-modeling study of the gas-phase oxidation of ammonia. React. Chem. Eng. 2020; 5, 696–711. https://doi.org/10.1039/C9RE00429G.

[64] Xi C, Fuller ME, Franklin GC. Decomposition kinetics for HONO and HNO 2. React Chem Eng 2019;4:323–33. https://doi.org/10.1039/C8RE00201K.

[65] Song Yu, Hashemi H, Christensen JM, Zou C, Marshall P, Glarborg P. Ammonia oxidation at high pressure and intermediate temperatures, Fuel 2016; 181, 358–65. DOI: 10.1016/j.fuel.2016.04.100.

[66] Valera-Medina A, Pugh DG, Marsh P, Bulat G, Bowen P. Preliminary study on lean premixed combustion of ammonia-hydrogen for swirling gas turbine combustors. Int J Hydrogen Energy 2017;42:24495–503. https://doi.org/10.1016/j.ijhydene.2017.08.028.

[67] Jiang X, Pan Y, Liu Y, Sun W, Huang Z. Experimental and kinetic study on ignition delay times of lean n-butane/hydrogen/argon mixtures at elevated pressures. Int J Hydrogen Energy 2017;42:12645–56. https://doi.org/10.1016/j.ijhydene.2017.03.196.

[68] Pan L, Hu E, Zhang J, Zhang Z, Huang Z. Experimental and kinetic study on ignition delay times of DME/H2/O2/Ar mixtures. Combust Flame 2014;161:735–47. https://doi.org/10.1016/j.combustflame.2013.10.015.

[69] Man X, Tang C, Wei L, Pan L, Huang Z. Measurements and kinetic study on ignition delay times of propane/hydrogen in argon diluted oxygen. Int J Hydrogen Energy 2013;38:2523–30. https://doi.org/10.1016/j.ijhydene.2012.12.020.

[70] Zhang Y, Huang Z, Wei L, Zhang J, Law CK. Experimental and modeling study on ignition delays of lean mixtures of methane, hydrogen, oxygen, and argon at elevated pressures. Combust Flame 2012;159:918–31. https://doi.org/10.1016/j.combustflame.2011.09.010.

[71] Herzler J, Naumann C. Shock-tube study of the ignition of methane/ethane/hydrogen mixtures with hydrogen contents from 0% to 100% at different pressures. Proc Combust Inst 2009;32:213–20. https://doi.org/10.1016/j.proci.2008.07.034.

[72] Gao X, Zhang Y, Adusumilli S, Seitzman J, Sun W, Ombrello T, et al. The effect of ozone addition on laminar flame speed. Combust Flame 2015;162:3914–24. https://doi.org/10.1016/j.combustflame.2015.07.028.

[73] Ombrello T, Won SH, Ju Y, Williams S. Flame propagation enhancement by plasma excitation of oxygen. Part I: Effects of O3. Combust Flame 2010;157:1906–15. https://doi.org/10.1016/j.combustflame.2010.02.005.

[74] Weng W, Nilsson E, Ehn A, Zhu J, Zhou Y, Wang Z, et al. Investigation of formaldehyde enhancement by ozone addition in CH4/air premixed flames. Combust Flame 2015;162:1284–93. https://doi.org/10.1016/j.combustflame.2014.10.021.

[75] Togun NK, Baysec S. Prediction of torque and specific fuel consumption of a gasoline engine by using artificial neural networks. Appl Energy 2010;87:349–55. https://doi.org/10.1016/j.apenergy.2009.08.016.

[76] Grosman B, Lewin DR. Automated nonlinear model predictive control using genetic programming. Comput Chem Eng 2002;26:631–40. https://doi.org/10.1016/S0098-1354(01)00780-3.

[77] Searson DP, Leahy DE, Willis MJ. GPTIPS: an open source genetic programming toolbox for multigene symbolic regression. In: Proceedings of the International multiconference of engineers and computer scientists 2010, IMECS 2010 I, pp 77–80.

[78] Searson D, Willis M, Montague G. Co-evolution of non-linear PLS model components. J Chemom 2007;21:592–603. https://doi.org/10.1002/cem.1084.
[79] Kumar P, Meyer TR. Experimental and modeling study of chemical-kinetics mechanisms for H2–NH3–air mixtures in laminar premixed jet flames. Fuel 2013; 108:166–76. https://doi.org/10.1016/j.fuel.2012.06.103.
[80] Wang N, et al. Laminar burning characteristics of ammonia/hydrogen/air mixtures with laser ignition. Int J Hydrogen Energy 2021;46:31879–93. https://doi.org/10.1016/j.ijhydene.2021.07.063.
[81] Di Sarli V, Benedetto AD. Laminar burning velocity of hydrogen–methane/air premixed flames. Int J Hydrogen Energy 2007;32:637–46. https://doi.org/10.1016/j.ijhydene.2006.05.016.
[82] Mitu M, Razus D, Schroeder V. Laminar burning velocities of hydrogen-blended methane–air and natural gas–air mixtures, calculated from the early stage of p(t) records in a spherical vessel. Energies 2021;14:7556. https://doi.org/10.3390/en14227556.